International Journal of Developmental Neuroscience 75 (2019) 44–58

Contents lists available at ScienceDirect

International Journal of Developmental Neuroscience

journal homepage: www.elsevier.com/locate/ijdevneu

Musashi-2 and related stem cell proteins in the mouse suprachiasmatic nucleus and their potential role in circadian rhythms

Dilshan H. Beligala[a], Arpan De[a], Astha Malik[b], Rae Silver[c,d], Kania Rimu[c], Joseph LeSauter[c], Hugh J. McQuillen[a], Michael E. Geusz[a,*]

[a] Department of Biological Sciences, Bowling Green State University, Bowling Green, OH, USA
[b] Division of Allergy and Immunology, Cincinnati Children's Hospital Medical Center, Cincinnati, OH, USA
[c] Department of Psychology, Barnard College, Columbia University, New York, NY, USA
[d] Department of Psychology, Columbia University, New York, NY, USA

ARTICLE INFO

Keywords:
Neural stem cell
Suprachiasmatic nucleus
Circadian rhythm
Neuroplasticity
RNA-binding protein
Astrocyte

ABSTRACT

Background: The suprachiasmatic nucleus (SCN) of the mammalian hypothalamus contains the master circadian clock of the body and an unusually large number of cells expressing stem cell-related proteins. These seemingly undifferentiated cells may serve in entrainment of the SCN circadian clock to light cycles or allow it to undergo neural plasticity important for modifying its rhythmic output signals. These cells may also proliferate and differentiate into neurons or glia in response to episodic stimuli or developmental events requiring alterations in the SCN's control of physiology and behavior.

Problem: To characterize expression of stem cell related proteins in the SCN and the effects of stem-like cells on circadian rhythms.

Methods: Explant cultures of mouse SCN were maintained in medium designed to promote survival and growth of stem cells but not neuronal cells. Several stem cell marker proteins including SRY-box containing gene 2 (SOX2), nestin, vimentin, octamer-binding protein 4 (OCT4), and Musashi RNA-binding protein 2 (MSI2) were identified by immunocytochemistry in histological sections from adult mouse SCN and in cultures of microdissected SCN. A bioinformatics analysis located potential SCN targets of MSI2 and related RNA-binding proteins.

Results: Cells expressing stem cell markers proliferated in culture. Immunostained brain sections and bioinformatics supported the view that MSI2 regulates immature properties of SCN neurons, potentially providing flexibility in SCN neural circuits. Explant cultures had ongoing mitotic activity, indicated by proliferating-cell nuclear antigen, and extensive cell loss shown by propidium iodide staining. Cells positive for vasoactive intestinal polypeptide (VIP) that are highly enriched in the SCN were diminished in explant cultures. Despite neuronal cell loss, tissue remained viable for over 7 weeks in culture, as shown by bioluminescence imaging of explants prepared from SCN of *Per1::luc* transgenic mice. The circadian rhythm in SCN gene expression persisted in brain slice cultures in stem cell medium. Prominent, widespread expression of RNA-binding protein MSI2 supported the importance of posttranscriptional regulation in SCN functions and provided further evidence of stem-like cells.

Conclusion: The results show that the SCN retains properties of immature neurons and these properties persist in culture conditions suitable for stem cells, where the SCN stem-like cells also proliferate. These properties may allow adaptive circadian rhythm adjustments. Further exploration should examine stem-like cells of the SCN in vivo, how they may affect circadian rhythms, and whether MSI2 serves as a master regulator of SCN stem-like properties.

Abbreviations: ABA, Allen Institute Mouse Brain Atlas; AHR, Aryl hydrocarbon receptor; AVP, arginine vasopressin; BLI, bioluminescence imaging; CLIP, cross-linking immunoprecipitation; DCX, doublecortin; DG, dentate gyrus; EGF, epidermal growth factor; FGF-2, fibroblast growth factor 2; FSS, Fine Structure Search; GFAP, glial fibrillary acidic protein; GO, Gene Ontology; GRP, gastrin-releasing peptide; HITS, high-throughput sequencing; HSC, mouse hematopoietic stem cells; ICC, immunocytochemistry; KD, knockdown; KO, knockout; MSI2, Musashi RNA-binding protein 2; NeuN, neuronal nuclei; NG2, neural/glial antigen 2; NSC, neural stem cell; Oct4, octamer-binding transcription factor 4; OE, overexpression; PCNA, proliferating cell nuclear antigen; RRM, RNA recognition motif; SCN, suprachiasmatic nucleus; SOX2, SRY-box containing gene 2; SPM, stem and progenitor cell culture medium; SVZ, subventricular zone; VIP, Vasoactive intestinal polypeptide

* Corresponding author. Dept. of Biological Sciences, Bowling Green State University, 217 Life Science Bldg, Bowling Green, OH 43403, USA.
E-mail address: mgeusz@bgsu.edu (M.E. Geusz).

https://doi.org/10.1016/j.ijdevneu.2019.04.007
Received 27 December 2018; Received in revised form 17 April 2019; Accepted 30 April 2019
Available online 03 May 2019
0736-5748/

1. Introduction

A fundamental question in brain development is what determines when individual brain regions lose their embryonic properties and mature. Cells with the characteristics of neural stem cells (NSCs) have been identified within the adult suprachiasmatic nucleus (SCN), a hypothalamic area containing a master circadian clock in many species, suggesting that this structure has characteristics of immature brain (Geoghegan and Carter, 2008). For example, Six3 genes show distinct expression in the SCN during early development, which persists in the adult (VanDunk et al., 2011). A role for these apparently immature cells in neurogenesis or the SCN's circadian rhythms remains unknown. Evidence suggests a low rate of neurogenesis persists in the adult hypothalamus (Migaud et al., 2015), while higher rates occur in the subventricular zone (SVZ) of the lateral ventricles and the hippocampal dentate gyrus (DG) of adult rodents (Yoo and Blackshaw, 2018). Recent studies also provide evidence that neurons serving in timing of ovulation are produced in pubertal and adult rat SCN and that adult neurogenesis in the SCN is important for female reproductive state (Mohr et al., 2017).

One possible function for the immature cell phenotypes of the SCN is that they may enable episodic neurogenesis providing SCN neural circuits a plasticity needed to modify circadian properties such as period, phase, or amplitude of rhythms. These alterations could compensate for events such as reproductive maturation, pregnancy, seasonal metabolic changes or other significant influences on circadian control of physiology and behavior. The SCN's unique role in regulating a wide range of behaviors and cellular processes, including sleep and daily metabolic cycles, and its adjustment to local time and seasonal conditions also suggest that it may rely on greater flexibility in its neural circuits compared to other hypothalamic areas of adult mammals (Migaud et al., 2015). The stem-like characteristics of SCN neurons and glia might also reflect a plasticity in cell interactions independent of complete neurogenesis because stem cells have mesenchymal cell properties including altered cell-cell contacts, morphological flexibility, and increased motility that could alter neural circuits (Zhao et al., 2016).

Evidence of the adult SCN's partially undifferentiated state includes cells expressing SOX2, an important regulatory protein in embryonic and adult neural stem cells (Hoefflin and Carter, 2014; Pellegrino et al., 2018), and doublecortin (DCX), a marker for immature cells such as neuroblasts committed to further differentiation into neurons (Walker et al., 2007; Geoghegan and Carter, 2008). DCX-expressing cells were described in the SCN's core region and co-localized with neurons expressing vasoactive intestinal polypeptide (VIP) or gastrin-releasing peptide (GRP)(Geoghegan and Carter, 2008). Also, the SCN has unusually low levels of NeuN (neuronal nuclei), a protein expressed in mature neurons, again revealing an immature feature possibly providing neuroplasticity (Geoghegan and Carter, 2008). Finally, doublecortin-like protein is expressed in the SCN along with DCX and has been implicated in neural plasticity (Saaltink et al., 2012). Proteins expressed during adult neurogenesis are well characterized in the mouse DG and SVZ, where NSCs replicate and differentiate into early progenitor cells that differentiate further into cells committed to becoming interneurons, astrocytes, or oligodendrocytes (Ming and Song, 2011). Stages of cell differentiation during adult neurogenesis are

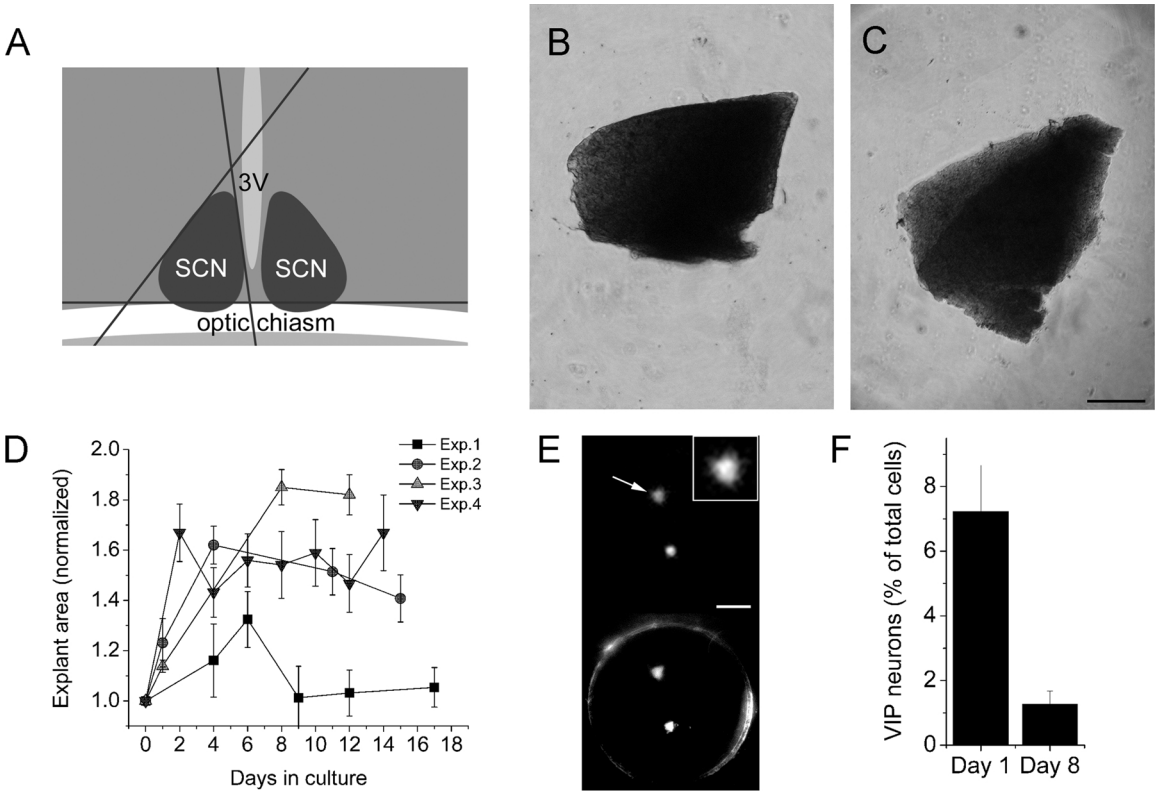

Fig. 1. SCN explant cultures in stem cell medium. Explants in SPM culture show tissue reorganization and cell movement. A: Where scalpel cuts were made in 300-μm-thick brain slices of the SCN region to remove the ependymal cells of the third ventricle (3 V) and the optic chiasm (OC). B: Explant at the start of culture. C: Same explant after 8 days in culture. Explant was made from a HRS mouse that was 64 weeks old. Scale bar = 50 μm. D: Cross-sectional area occupied by explants providing a measure of tissue reorganization in SPM. Shown are average areas (± SEM) for explants in four experiments (25 explants). Mean explant area increased significantly between days 1 and 6 (T test, t = 5.641, p = 0.011, n = 4 experiments). E: Bioluminescence imaging of explants expressing luciferase under control by the Per1 gene promoter. Bottom: Corresponding brightfield image. Explants were in culture for 52 days and were made from a 38 week-old B6 (*Per1::luc*) mouse. F: Loss of neurons in SCN explants with time in culture in SPM while circadian clock gene expression persists. Explant has significantly fewer VIP-positive cells ($p < 0.001$) after 8 days in culture.

distinguished by their unique protein expression patterns (von Bohlen Und Halbach, 2007).

Immunocytochemistry was used in the present study to test for these and other protein markers of stem cells in microdissected SCN explants prepared from juvenile and adult mice. A stem and progenitor cell culture medium (SPM) was used that maintains stem-like properties while suppressing differentiation and promoting NSC growth. We examined whether SCN stem-like cells survive and proliferate under these conditions. This physiological property of stem-like cells was combined with immunostaining results characterizing the surviving cells. Immunostained brain sections and SCN explants revealed stem cell markers OCT4, nestin, and RNA-binding protein MSI2 in mouse SCN. The results indicated a latent SCN ability that may be activated in response to physiological challenges or individual life events.

We also addressed whether SCN circadian rhythms persist in SPM. Previously, circadian rhythms appeared lacking in NSCs of neurosphere cultures prepared from adult mouse SVZ and DG until they were induced to differentiate (Malik et al., 2015a, b). We report that this minimal culture medium not only supported cell survival and proliferation but also permitted neurons or glial cells to express circadian rhythms that persisted with distinct modulation. In addition, a bioinformatics study centered on MSI2, which is highly expressed in the SCN (Beligala et al., 2018), supported the view that immature properties of SCN neurons allow a coordinated flexibility in its neural circuits, possibly facilitating adaptive circadian rhythm adjustments.

2. Materials and methods

2.1. Animals

Mice were bred and maintained in cycles of 12 h light and 12 h dark to entrain their circadian system. Food and water were provided ad libitum. Males and females of three mouse strains were used to evaluate how broadly stem-like cells occur in the SCN: C57BL/6 (B6), C3H, and HRS. Some B6 and HRS mice contained the *Per1::luc* transgene, and some C3H mice contained a *fos::luc* transgene. Only bioluminescence from *Per1::luc* tissue was used in this study. Animals were 3–72 weeks old at the time of tissue harvesting, except where noted. Animal procedures were approved by the Institutional Animal Care and Use Committees of BGSU and Columbia University and met National Institutes of Health guidelines.

2.2. Microdissected SCN explant cultures and immunocytochemistry (ICC)

For immunocytochemistry (ICC) of SCN immediately after sectioning, 150 µm-thick coronal sections were made from ice-chilled brains removed after isoflurane anesthesia. For SCN explant cultures, surgical reductions of each SCN in 300-µm coronal brain sections were made with three scalpel cuts to remove the ependymal cell layer and optic chiasm tissue as shown in Fig. 1A. Explants were placed in glass-bottom culture dishes (Mattek) or plastic culture dishes, containing SPM, which consisted of Dulbecco's Modified Eagle Medium (DMEM) with 10 ng/ml fibroblast growth factor-2 (FGF-2, Invitrogen), 20 ng/ml epidermal growth factor (EGF, Invitrogen) and 100 U/ml penicillin and 100 µg/ml streptomycin. SPM lacks many of the growth factors and other differentiation-inducing agents of standard serum-based cultures or medium used with various serum supplements to maintain neuron survival in vitro.

Bright field microscope images were captured at 2-day intervals with a 4X lens and a megapixel Kodak digital color camera. For immunofluorescence imaging, explants in culture for 11–32 days (average of 16 days) were fixed in 100% methanol for 10 min or 4% formalin in phosphate-buffered saline for 1 h at room temperature (RT) and standard ICC was performed. Indirect immunofluorescence staining with confocal microscopy was used to identify stem-like cells, neurons, astrocytes, and proliferating cells. Samples were rinsed after overnight incubation at 4 °C with primary antibodies and were then incubated for 2 h with appropriate Alexa Fluor 488 and Alexa Fluor 568-conjugated secondary antibody (Life Technologies) at room temperature on a shaker. Confocal microscopy was performed as described in our previous study of neurosphere cultures (Malik et al., 2015a, b). ICC was also performed using mice after transcardial perfusion with formaldehyde 2 h after lights on. Cryostat sections were incubated with mouse anti-GFAP (glial fibrillary acidic protein) and rabbit anti-MSl2 antibodies and stained with Cy2 anti mouse and Cy3 anti-rabbit (Table 1).

Confocal microscopy was performed as described previously (Malik et al., 2015a), Briefly, cells were imaged with a DMI3000B inverted microscope (Leica Microsystems, Buffalo Grove, IL, USA) equipped with a Spectra X LED light engine (Lumencore, Beaverton, OR, USA), X-Light spinning-disk confocal unit (CrestOptics, Rome, Italy), and a Rolera Thunder cooled − CCD camera (Photometrics) with Metamorph software controlling image acquisition and data analysis (Molecular Devices, Sunnyvale, CA, USA). Confocal images were collected in a Z-series with 10X and 20X objectives while using standard DAPI, fluorescein, and rhodamine filter wavelengths. The distribution of cell types was then determined and cell counts were obtained using Metamorph Multi-Wavelength Cell Scoring Application Module after background intensity was subtracted based on the highest intensity measurements from controls in which primary antibody was omitted. Cells having a brightness within the top 75% of the intensity range were counted as positive. For Fig. 2E, 50 µm sagittal sections containing the SCN were photographed with a Nikon Eclipse E800 microscope equipped with a cooled CCD camera (Retiga Exi; Q-Imaging), using Q-capture software. For Fig. 3, the same section was observed under a Zeiss Axiovert 200 MOT fluorescence microscope (63× objective) with a Zeiss LSM 510

Table 1
List of primary antibodies used.

Product name	Target	Catalog number	Supplier	Working concentration	Monoclonal/ polyclonal
mouse anti-GFAP	GFAP	3670	Cell Signaling Technology	1:1000	Monoclonal
mouse anti-GFAP	GFAP	sc-33673	Santa Cruz Biotechnology	1:500	Monoclonal
mouse anti-GFAP	GFAP	sc-33673	Santa Cruz Biotechnology	1:1000	Monoclonal
rabbit anti-MSI2	Musashi2	PA5-21145	Invitrogen	1:200	Polyclonal
rabbit anti-MSI2	Musashi2	10770-1-AP	Proteintech	1:250	Polyclonal
chicken anti-nestin	nestin	NES	Aves Labs	1:1000	Polyclonal
chicken anti-NeuN	NeuN	NUN	Aves Labs	1:1000	Polyclonal
mouse anti-NG2 (neural/glial antigen 2)	NG2	sc-53389	Santa Cruz Biotechnology	1:200	Monoclonal
rabbit anti-Oct-4	Oct-4	A7920	Abclonal	1:500	Polyclonal
mouse anti-PCNA	PCNA	sc-25280	Santa Cruz Biotechnology	1:500	Monoclonal
rabbit anti-SOX2	SOX2	48-1400	Life Technologies	1:500	Polyclonal
mouse anti-vimentin	vimentin	sc-373717	Santa Cruz Biotechnology	1:500	Monoclonal
rabbit anti-VIP	VIP	A1804	Neo Scientific	1:100	Polyclonal
rabbit anti-VIP	VIP	A1804	Abclonal	1:500	Polyclonal

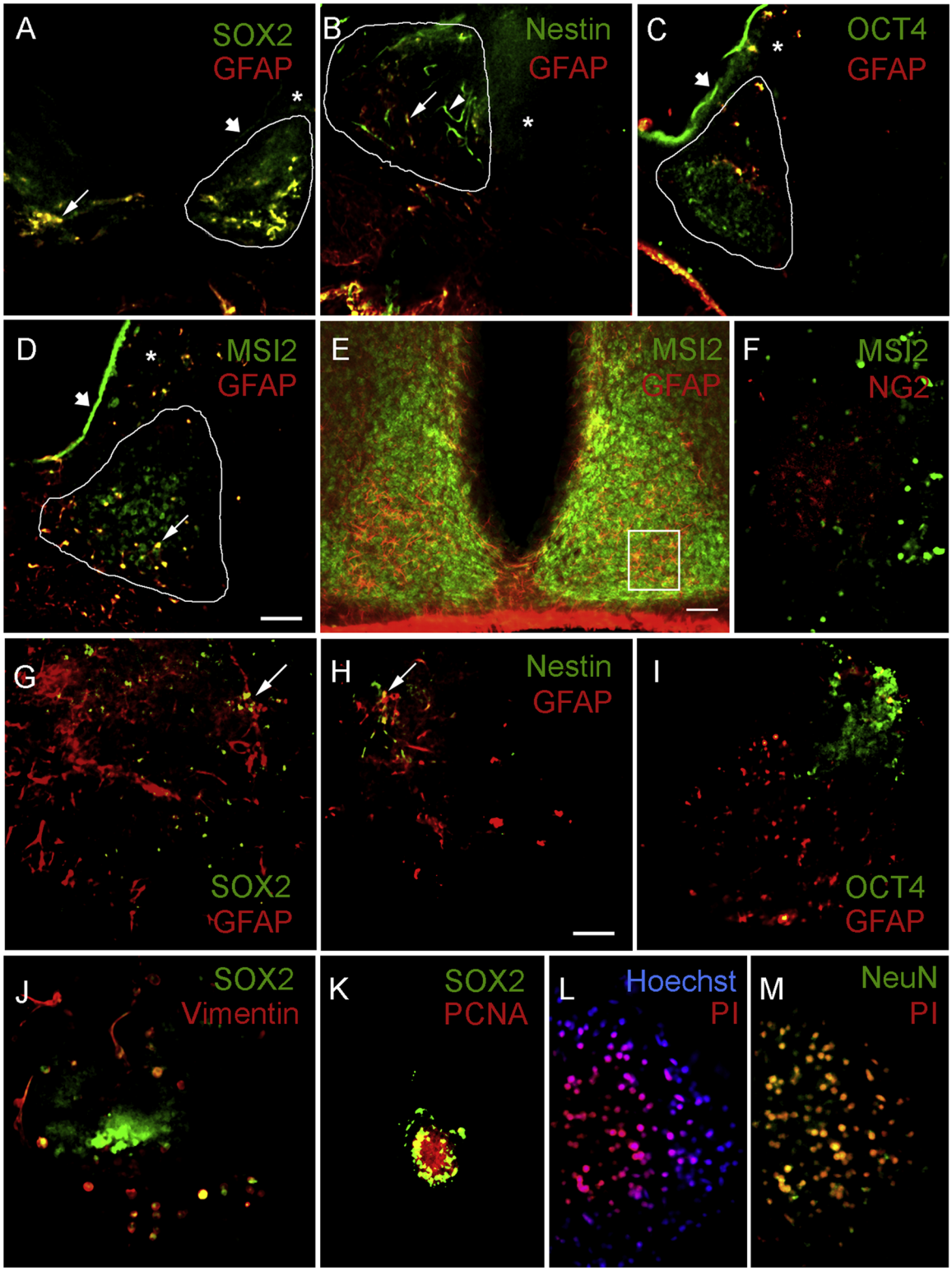

Fig. 2. Stem cell markers provide additional evidence of neural stem cells and progenitor cells in the SCN and SCN explant cultures. Immunocytochemistry of brain slices containing SCN and surrounding hypothalamus fixed immediately after sectioning show A: SOX2, B: Nestin, C: OCT4, and D: MSI2 expression (green) along with GFAP + cells (red). Arrows: colocalization with GFAP (yellow). Clusters of SOX2+/GFAP + and nestin+/GFAP + cells resembling stem cells (yellow) are near the explant core. SCN outline indicates the region used for cell counting. Asterisk: location of neighboring hypothalamic regions dorsal or lateral to SCN for comparison. Arrowhead: blood capillaries positive for nestin. Scale bar = 100 µm. E: Ex-vivo coronal sections show that MSI2 expression (green) is distributed throughout the SCN along with GFAP expression (red). (Rectangle: region expanded in Fig. 3) F: MSI2 expression (green) in SCN explant cultures does not colocalize with neuroglial cells expressing NG2 (red). SCN explant cultures contain cells expressing G: SOX2 (green), H: nestin (green), and I: OCT4 along with GFAP + cells (red). Arrows: colocalization with GFAP. J: SOX2 (green) and additional stem cell marker vimentin (red) show colocalization in SCN explants. K: Cell division occurs throughout SCN explants (PCNA+, red), which includes SOX2+ cells primarily near the edge (yellow). Some SOX2+ cells appear to be quiescent (green). L: Cell death is mostly near the center of SCN explants (red: propidium iodide; blue: Hoechst-stained cell nuclei). M: In the same explant, it is clear that mostly neurons (NeuN+) are undergoing cell death (orange and yellow), and few neurons survive (green). Scale bars: 100 µm in A–E and I–K, but 50 µm elsewhere (For interpretation of the references to colour in this figure legend, the reader is referred to the web version of this article).

laser scanning confocal attachment (Carl Zeiss). The sections was excited with argon-krypton, argon, and helium-neon lasers using the excitation wavelengths of 488 nm for Cy2, 543 nm for Cy3, and 633 nm for Cy5. Each laser was excited sequentially to avoid cross talk between the three wavelengths.

2.3. Live/Dead staining

Cultures were incubated in 0.02 mg/ml propidium iodide (PI) in PBS for 5 min at 37 °C. PI was then washed out using PBST (0.1% Triton in PBS), and cells were fixed using 100% methanol for 10 min at RT. Explants were washed with PBS, and cell nuclei were stained using Hoechst 334 before confocal fluorescence imaging, as described previously (Malik et al., 2015b).

2.4. Explant bioluminescence imaging

Culture dishes containing surgically reduced SCN explants in serum-containing medium (SM) consisting of DMEM and 10% FBS were covered with a temperature-controlled optical window, sealed with silicone grease, and maintained at 37 °C (Cell MicroControls, Norfolk, VA). Luciferin, potassium salt (0.5 mM), was added to explants before imaging with a back-thinned, back-illuminated CCD camera (CH360, Photometrics, Tucson, AZ) or Retiga LUMO cooled CCD camera (QImaging). These long-term brain slice cultures were imaged with 60-min exposures. Bioluminescence imaging (BLI) of explants was performed with 2 × 2 binning and 30-min exposures. Images were analyzed using V++ (Photometrics) and ImageJ (NIH) software.

BLI was also performed with standard brain slice explant cultures of the SCN maintained in SPM for only 8–10 h and then maintained in a modified SPM during BLI. For BLI, bicarbonate was reduced to 4 mM for use in room air, and 10 mM HEPES buffer was used to maintain pH at 7.2. Pen/strep was added and no phenol red was used, as with cultures in 5% CO_2.

Coronal brain sections, 300 μm-thick, were prepared from male mice 38–123 days old using the same procedure as explant cultures but, because of their larger size, were placed on Millipore cell culture inserts with a thin film of medium (1 ml total) covering the tissue in a 35 mm plastic cell culture dish, as described previously (Hiler et al., 2008).

2.5. Bioinformatics analysis

The most likely MSI2 targets were derived from published high-throughput crosslinking immunoprecipitation (CLIP) and gene expression data generated after knockout (KO), knockdown (KD) or overexpression (OE) of Msi2 in mice or various cell types (Wu et al., 2010; Park et al., 2014; Wang et al., 2015; Bennett et al., 2016; Rentas et al., 2016; Kharas and Lengner, 2017). Data from in situ hybridization (ISH) experiments using sections from adult mouse brain were obtained from the Allen Institute Mouse Brain Atlas (ABA) and are available online at http://mouse.brain-map.org (Lein et al., 2007). To generate Table 2, the Fine Structure Search (FSS) tool for the ABA was used that provided a curated list of the 46 most significantly expressed SCN genes according to ISH intensity and degree of selective expression in the SCN. FSS genes were added to Table 2 if one or more of these criteria were met: (1) The gene's RNA is a likely target of MSI2 regulation, negative or positive, based on CLIP or gene expression studies; (2) The gene product is reported to bind to or otherwise interact directly with MSI2; or (3) has high SCN expression (z-score > 1) based on ISH ABA reported results (i.e., the signal is more than one standard deviation from the mean of all observed SCN gene expression).

Additional genes were included in Table 2 if (1) the gene product is in the RBM family of RNA-binding proteins along with MSI2; (2) was examined in this study through ICC; or (3) is an additional gene discussed in this report in relation to stem cells or cell-cell contact. The estimated period of any circadian rhythm in gene expression described in the SCN was added if it was available in the CircaDB database of microarray results. For each gene, up to two GO codes were selected, if available, based on biological functions in this order: (1) neuronal or glial activity including circadian rhythm functions; (2) stem cells or developmental processes; (3) RNA binding; and (4) other processes closely related to developmental processes such as cell division, cell-cell contact or apoptosis.

Gene Ontology (GO) designations were obtained from the Mouse Genome Informatics (MGI) database at http://www.informatics.jax.org/batch/summary. For high stringency, only Experimental, Computational Analysis, and Curator Statement Evidence Codes were used in Table 2, except in one case when these were not available and the Inferred from Electronic Annotation (IEA) Evidence Code was used instead. Estimates of circadian rhythms in gene expression in the mouse SCN were obtained from the database CircaDB using default search criteria, which is available at http://circadb.hogeneschlab.org (Pizarro et al., 2013).

3. Results

3.1. Culture in SPM causes morphological and cellular changes in SCN explants

Explants were prepared from brain slices that were surgically-reduced by microdissection to remove the optic chiasm and ependymal cells along with the ventricular zone as shown in Fig. 1A, thereby eliminating these possible sources of stem-like cells from outside the SCN. During culture in SPM, explants showed distinctive changes in morphology and tissue rearrangement including a transient, 29.1% increase in cross-sectional area (Fig. 1B-D) as cells were proliferating or dying. Although the explants were maintained in a medium that does not favor growth and survival of differentiated cells, cultures remained

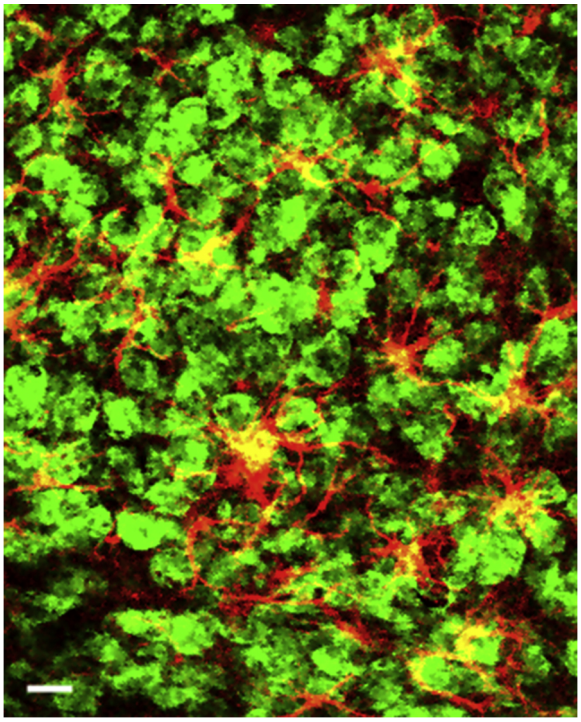

Fig. 3. Cells expressing MSI2 and GFAP in SCN. The photomicrograph presents a high magnification view of the inset in Fig. 2E showing fine details of fibrous astrocytes expressing MSI2 (green) and GFAP (red) in sections of fixative-perfused mouse brain. Neighboring GFAP-negative cells also express MSI2 and are in close proximity to astrocyte processes. Confocal image is a 1-μm Z-axis optical section. Scale bar: 10 μm (For interpretation of the references to colour in this figure legend, the reader is referred to the web version of this article).

Table 2
RNA-binding, circadian, and stem cell properties of selected genes expressed in mouse SCN.

Gene	Contains RBM	MSI2-binding or control	Relative expression level (Z score)	Present in SCN FSS	Selected gene ontology (GO Biological Process)	SCN circadian rhythm period (hrs)
Blcap (Bladder cancer-associated protein), 71016617	–	Bennett et al. (2016)	3.000	+	GO:0030262 apoptotic nuclear changes	20.0-24.0
Celf3 (CUGBP, Elav-like family member 3), 74641324	+	–	1.994	+	GO:0007283 spermatogenesis GO:0000381 regulation of alternative mRNA splicing, via spliceosome	24.0
Celf4 (CUGBP, Elav-like family member 4), 73592527	+	–	1.154	–	GO:0090394 negative regulation of excitatory postsynaptic potential GO:1902866 regulation of retina development in camera-type eye	24.0
Celf6 (CUGBP, Elav-like family member 6), 71358616	+	–	1.676	–	GO:0001505 regulation of neurotransmitter levels GO:0071625 vocalization behavior	ND
Cirbp (cold inducible RNA binding protein), 69548958 sagittal	+	Park et al. (2014); Rentas et al. (2016)	< 1	–	GO:0045727 positive regulation of translation GO:0030308 negative regulation of cell growth	(24.0)[1]
Dclk1 (doublecortin-like kinase 1, Dcl), 69169654 sagittal	–	–	< 1	–	GO:0048813 dendrite morphogenesis GO:0021952 central nervous system projection neuron axonogenesis	24.0
Dcx (doublecortin), 70946414 sagittal	–	–	< 1	–	GO:0001764 neuron migration GO:0021952 central nervous system projection neuron axonogenesis	24.0
Dlk1 (delta-like 1 homolog), 71587885	–	–	< 1	+	GO:0030154 cell differentiation GO:0045746 negative regulation of Notch signaling pathway	ND
Dlx1 (distal-less homeobox 1), 72008490 and 348	–	–	< 1	+	GO:0021892 cerebral cortex GABAergic interneuron differentiation GO:0045746 negative regulation of Notch signaling pathway	24.0
Dner (delta/notch-like EGF-related receptor), 1699	–	–	< 1	–	GO:0010001 glial cell differentiation GO:0005112 Notch binding	ND
Elav1 (embryonic lethal, abnormal vision 1), None	+	Rentas et al. (2016)[2]	< 1	–	GO:2000036 regulation of stem cell population maintenance GO:0045727 positive regulation of translation	24.0
Flrt3 (fibronectin leucine rich transmembrane protein 3), 73931404	–	Bennett et al. (2016)	3.08	+	GO:0051965 positive regulation of synapse assembly GO:0098742 cell-cell adhesion via plasma-membrane adhesion molecules	24.0
Gfap (glial fibrillary acidic protein), 79591671 and 1357	–	–	2.432[1]	–	GO:0010977 negative regulation of neuron projection development GO:0045109 intermediate filament organization	ND[3]
Msi1 (musashi RNA-binding protein 1), 74509595 sagittal	+	–	< 1	–	GO:0003727 single-stranded RNA binding GO:0008266 poly(U) RNA binding	ND
Msi2 (musashi RNA-binding protein 2), 73616034	+	Rentas et al. (2016)	2.117	+	GO:0048864 stem cell development GO:0008266 poly(U) RNA binding	ND
Nes (nestin), 1387	–	–	1.501	–	GO:0007399 nervous system development GO:0048858 cell projection morphogenesis	ND
Notch1, 70593326 sagittal	–	Park et al. (2014)	< 1	–	GO:0050768 negative regulation of neurogenesis GO:0010718 positive regulation of epithelial to mesenchymal transition	ND
Notch2, 69837872 sagittal	–	Bennett et al. (2016)	< 1	–	GO:0001709 cell fate determination GO:0007219 Notch signaling pathway	ND
Ntpcr (nucleoside-triphsphatase, cancer-related), 75773704	–	Rentas et al. (2016)	2.113	+	GO:0005524 ATP binding[4] GO:0098519 nucleotide phosphatase activity, acting on free nucleotides[4]	ND
Numb, 69095946 sagittal	–	Rentas et al. (2016)	< 1	–	GO:0050769 positive regulation of neurogenesis GO:0045746 negative regulation of Notch signaling pathway	ND
Pdcd4 (programmed cell death 4), 73931413	–	Rentas et al. (2016)	1.533	+	GO:1905064 negative regulation of vascular smooth muscle cell differentiation GO:0060940 epithelial to mesenchymal transition involved in cardiac fibroblast development	28
Pou2f1 (POU domain, class 2, transcription factor 1) (OCT1), 1563	–	Rentas et al. (2016)	1.752	–	GO:0030910 olfactory placode formation GO:0045944 positive regulation of transcription by RNA polymerase II	ND
Pou5f1 (POU domain, class 5, transcription factor 1, OCT 4), 71325348 sagittal	–	–	< 1	–	GO:0019827 stem cell population maintenance GO:0035198miRNA binding	ND
Rbfox2, 71325402 sagittal	+	Rentas et al. (2016)	< 1	–	GO:0048813 dendrite morphogenesis GO:0000381 regulation of alternative mRNA splicing, via spliceosome	24
Rbfox3 (NeuN), None	+	–	ND[5]	–	GO:0007399 nervous system development GO:0000381regulation of alternative mRNA splicing, via spliceosome	ND[6]
Rbm4 (RNA Binding Motif Protein 4; Lark1), 888	+	Rentas et al. (2016)	1.534	–	GO:0097167 circadian regulation of translation GO:0043153 entrainment of circadian clock by photoperiod	ND[7]

(*continued on next page*)

Table 2 (*continued*)

Gene	Contains RBM	MSI2-binding or control	Relative expression level (Z score)	Present in SCN FSS	Selected gene ontology (GO Biological Process)	SCN circadian rhythm period (hrs)
Rgs16 (regulator of G-protein signaling), 1567	–	Rentas et al. (2016)	< 1	+	GO:0007186 G-protein coupled receptor signaling pathway GO:0043547 positive regulation of GTPase activity	24.0-28.0
Rnpc3 (RNA binding region (RNP1, RRM) containing 3), 583856 sagittal	+	–	< 1	–	GO:0032502 developmental process GO:0000398 mRNA splicing, via spliceosome	ND
Rorb (RAR-related orphanreceptor beta), 2539 and 79556597	–	Rentas et al. (2016)	–	+	GO:0042752 regulation of circadian rhythm GO:0042462 eye photoreceptor cell development	24.0
Rps6ka2 (ribosomal protein S6 kinase, polypeptide 2), 70301276	–	Rentas et al. (2016)	< 1	+	GO:0002035 brain renin-angiotensin system GO:0007507 heart development	ND
Shh (sonic hedgehog), 1418	–	Ma et al. (2017)	8.543	–	GO:0007417 central nervous system development GO:0030178 negative regulation of Wnt signaling pathway	ND
Slc5a3 (solute carrier family 5 (inositol transporters), member 3), 976	–	Bennett et al. (2016)	3.356	+	GO:0007422 peripheral nervous system development GO:0045746 negative regulation of Notch signaling pathway	24.0
Sox2 (SRY-box containing gene 2), 77280331	–	Coexpressed with Msi2[8]	5.289	+	GO:0045747 positive regulation of Notch signaling pathway GO:0035198 miRNA binding	ND
Ssb (Sjogren syndrome antigen B, La), 75081397	+	Bennett et al. (2016); Rentas et al. (2016)	< 1	–	GO:1990825 sequence-specific mRNA binding GO:0071045 nuclear histone mRNA catabolic process	ND
Syncrip (synaptotagmin binding, cytoplasmic RNA interacting protein, hnRNP Q), 1391	+	Wang et al. (2015); Bennett et al. (2016); Rentas et al. (2016)	< 1	–	GO:0008143 poly(A) binding GO:0017148 negative regulation of translation	ND
Trp53i11 (transformation related protein 53 inducible protein 11), 73521826	–	Bennett et al. (2016); Rentas et al. (2016)	3.696	+	GO:0016021 integral component of membrane[4]	ND
Vim (vimentin), 1309 and 79907904	–	–	1.921	–	GO:0014002 astrocyte development GO:0010977 negative regulation of neuron projection development	ND
Wnt2b (wingless-related MMTV integration site 2B), 1589	–	Kharas and Lengner (2017)	5.444	–	GO:0030182 neuron differentiation GO:0045165 cell fate commitment	ND
Wnt10b, 2725	–	Kharas and Lengner (2017)	4.382	–	GO:0030182 neuron differentiation GO:0071425 hematopoietic stem cell proliferation	ND
Zfhx3 (zinc finger homeobox 3), 74641308	–	Rentas et al. (2016)	4.875	+	GO:0032922 circadian regulation of gene expression GO:0045662 negative regulation of myoblast differentiation	ND[9]

Gene: names followed by the Allen Mouse Brain Atlas experiment number for coronal sections, except where indicated. Boldfaced genes indicate where protein expression was confirmed in brain sections or tissue explants during the current study. Contains RBM: RRM domain present in protein. MSI2-binding or controlled: based on published studies. Relative expression level: number of standard deviations above the average expression of genes in SCN, from ISH data in the Allen Institute Mouse Brain Atlas and Brain Explorer. Present in SCN FSS: from Fine Structure Search of SCN by Allen Institute using Mouse Brain Atlas. Selected gene ontology: from MGI database. SCN circadian rhythm: CircaDB JTK analysis with $p > 0.05$, default settings; ND = not detected. [1]Average of two experiments. [2]ELAVL1 binds RNA along with MSI2 and is upregulated by MSI2 KO (Park et al., 2014). [3]SCN astrocytes show daily rhythms in GFAP cell localization (Lindley et al., 2008). [4]Only available GO is from IEA (Inferred from Electronic Annotation). [5]Not detected in ABA; published results show low expression in SCN cells. [6]E-box in Rbfox3 gene promoter could provide circadian clock control. [7]LARK protein levels show circadian rhythm modulation (Kojima et al., 2007). [8](Cox et al., 2013) [9]Long (32-hr) period detected. MSI-2-binding results were derived from several studies of MSI2 KO, KD or overexpression (Wu et al., 2010; Park et al., 2014; Wang et al., 2015; Bennett et al., 2016; Rentas et al., 2016; Kharas and Lengner, 2017).

viable, as shown by bioluminescence imaging of explants prepared from SCN of *Per1::luc* transgenic mice after 52 days in culture (Fig. 1E). The explants showed a loss of neurons expressing VIP, which comprise a major cell population in the SCN (Fig. 1F, Supplemental Fig. 1).

3.2. SCN cells express multiple stem cell-related proteins

ICC provided additional evidence of stem-like cells in the SCN by applying antibodies directed against SOX2, nestin, OCT4, MSI2, and GFAP in brain sections that were formalin-fixed immediately after sectioning (Fig. 2A-D, Fig. 3). This approach is similar to ICC methods used to characterize cell types in SCN slice cultures (Iwai and Takeda, 2007) and it shows the state of cells in explant cultures before circadian rhythms are measured, which is described below. GFAP ICC was used to identify putative stem cells, astrocytes and, more effectively, reactive astrocytes (Sofroniew and Vinters, 2010), which are considered to have neurogenesis capabilities in cerebral cortex (Robel et al., 2011; Magnusson et al., 2014; Michelucci et al., 2016).

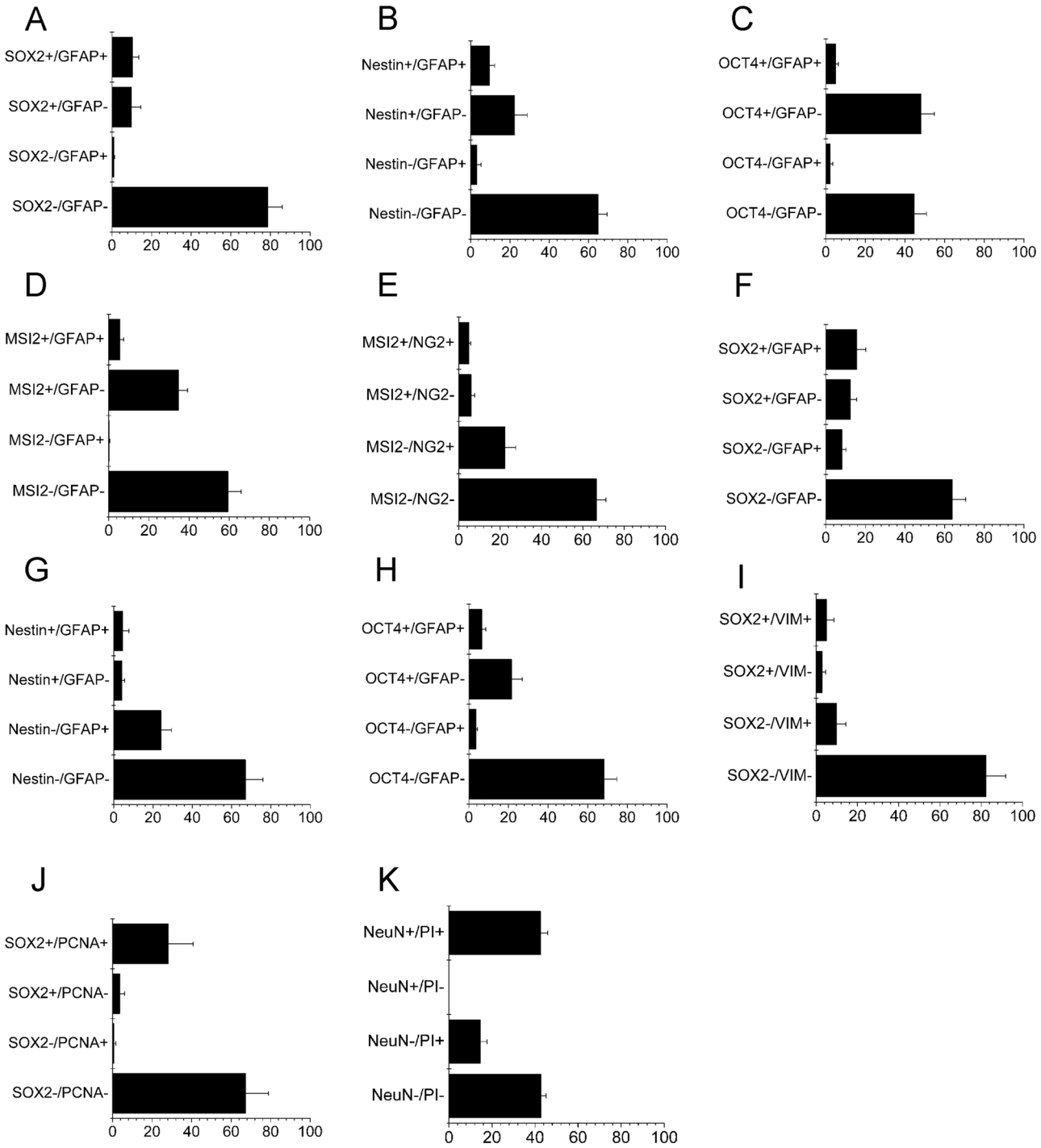

Fig. 4. Proportions of cells expressing stem cell proteins in the SCN and SCN explant cultures. Percentages are relative to total cells identified by Hoechst-stained nuclei in one confocal section. Percentages of cells expressing stem cell markers; SOX2 (a), Nestin (b), OCT4 (c) and MSI2 (d) in the SCN in brain slices fixed immediately after sectioning (average of 4 SCNs). Percentages of cells expressing stem cell markers; MSI2 (e) SOX2 (f), Nestin (g) and OCT4 (h) in the SCN explant cultures (average of 5 locations in one explant). Percentages of cells expressing a mesenchymal cell marker vimentin with SOX2 (i), a cell proliferation marker PCNA with SOX2 (j) and an apoptotic nuclear stain PI with a neuronal marker NeuN (k) in SCN explant cultures (average of 5 locations in one explant).

In all brain sections examined, GFAP was more commonly expressed in cells containing SOX2, Nestin, OCT4 or MSI2 than in cells that did not express these stem cell-related proteins (Fig. 4A-D). SOX2 was expressed about equally in GFAP-negative and positive cells (Fig. 4A), consistent with reports of its expression in both SCN neurons and glia (Hoefflin and Carter, 2014). The brain sections were prepared immediately after dissection and chilled on ice before fixarion so that immunostaining could be compared directly with results from the SCN explant cultures, as shown by Liu et al., 2018 (Liu et al., 2018). However, MSI2 was examined in both non-perfused sections and ones made

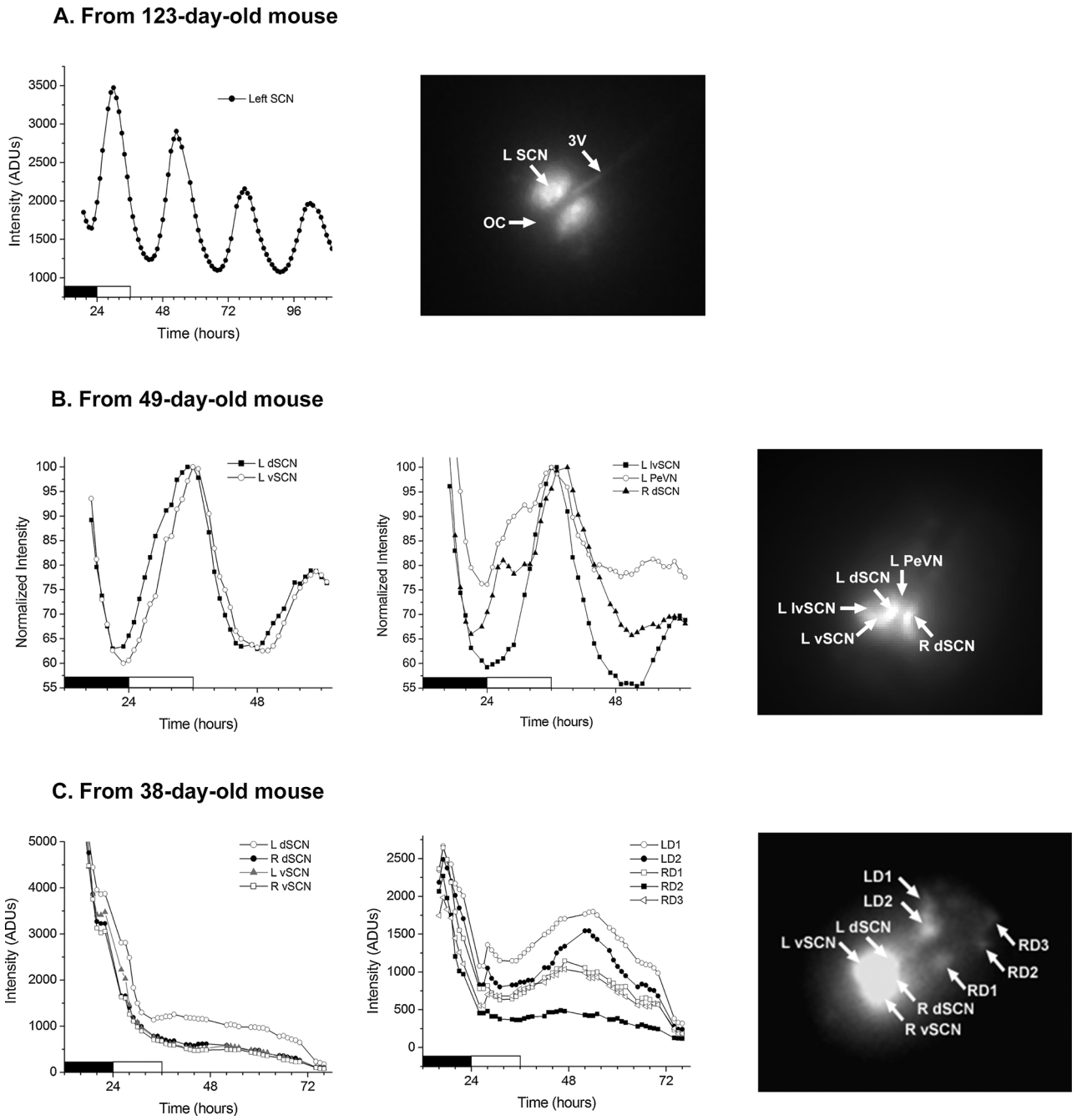

Fig. 5. Bioluminescence imaging of SCN brain slices maintained in SPM. A: SCN brain slice prepared from a 123-day-old *Per1::luc* transgenic mouse. Left: Circadian bioluminescence rhythm measured from the entire left SCN signal. Right: Bioluminescence image captured 12 h after imaging began showing signal originating almost entirely from the paired SCN. The circadian rhythms and expression pattern were typical of previously described SCN brain slices in normal culture medium. L SCN: left SCN. 3 V: third ventricle. OC: optic chiasm. The timing of the prior light/dark cycle is shown below. ADUs: analog-to-digital units of the sensor after background subtraction. B: SCN brain slice from a 49-day-old *Per1::luc* mouse. Left: Circadian expression in the SCN persisted in the left SCN with the dorsal SCN (L dSCN) slightly preceding the ventral SCN (L vSCN), as described previously in SCN imaged under normal culture conditions. A circadian rhythm was also detected near the lateral edge of the left ventral SCN (L lvSCN). The periventricular nucleus (L PeVN) showed unusually high and sustained expression. Right: A circadian rhythm was also present in the right SCN, although the pattern included a smaller peak occurring 12 h earlier than the maximum. Arrows indicate centers of each region-of-interest (ROI). Bioluminescence signals shown were normalized to the maximum in each ROI to facilitate phase comparisons. C: SCN brain slice from 38-day-old *Per1::luc* mouse. Rhythms in both SCN were disrupted within the first cycle in vitro. Left: Signals recorded from ROIs in the left (L) and right (R) dorsal SCN (dSCN) and ventral SCN (vSCN) as indicated by arrows shown at right. Expression in other areas increased over time, particularly in spots lateral to the third ventricle (3 V). Left dorsal areas (LD1, LD2) and right dorsal areas (RD1, RD2. RD3) showed increased expression late during the recording and were not rhythmic.

from formalin-perfused brains as shown in 50 um sections of SCN (Fig. 2E, Fig. 3). MSI2 staining intensity was elevated in the SCN relative to surrounding hypothalamic tissue and was expressed throughout the shell and core SCN subregions. Confocal microscopy indicated that most, if not all, GFAP-immunoreactive cells contain MSl2 and are widely distributed between other cell types (Fig. 3).

3.3. SCN explant cultures express stem cell and progenitor cell markers

As in brain slices, SOX2, nestin, and OCT4 were co-expressed with GFAP in SCN explant cultures after 1–4 weeks in SPM (Fig. 2G-I). The percentage of GFAP-positive cells was significantly higher in explants than in brain slices (20.9% ± 9.62 SD, n = 3 explants versus 9.31% ± 3.35, n = 4 slices, p = 0.035, t-test). Cell counts within five regions were averaged for each slice or explant. This result suggests that reactive astrocytes (potential stem-like cells) were induced or proliferated in SCN explants.

SOX2 in explant cultures was also co-expressed with vimentin (Fig. 2J), a marker for cells that have undergone epithelial-to-mesenchymal transition (EMT) through a dedifferention process that generates stem-like cells (Nie et al., 2009). MSI2 was observed in explant cultures and did not show expression in neuroglial cells, another cell type that survived in SPM (Fig. 2F).

Cells proliferating or undergoing cell death were quantified in explant cultures by PCNA ICC (Fig. 2K) and PI staining (Fig. 2L), respectively. Nearly all SOX2-positive cells in explants were undergoing mitosis according to PCNA staining (88%, Fig. 4J). PI was applied prior to fixation to identify cells with compromised cell membranes. About 74% of PI-labeled cells expressed NeuN, and all NeuN-positive cells examined were PI stained (Fig. 2L, M), further confirming a major loss of neurons in SPM. The percentages of cells positive for nestin, OCT4, and MSI2 were lower in explants than in brain slices, possibly because most of these cells were GFAP-negative in brain slices (Fig. 4B-D) and therefore likely included neurons that did not survive in explant cultures.

3.4. Bioinformatics indicate significant MSI2 and RNA-binding protein functions in SCN

The extensive MSI2 expression in the SCN detected by ICC encouraged further examination of this RNA-binding protein that suppresses differentiation of stem cells and is expressed in the DG and SVZ (Sakakibara et al., 2001). The MSI2 expression pattern, which was distributed across the SCN in brain sections, agreed with the Msi2 gene expression pattern in the ABA based on ISH in coronal and sagittal sections. This feature suggests it may have an important function in multiple SCN activities including circadian rhythm generation, entrainment of the clock to retinal input, and distribution of rhythmic timing signals. The gene ontology (GO) bioprocess (BP) annotation in PANTHER indicates MSI2 regulates RNA metabolic processes and serves in stem cell development. The other member of the Musashi gene family, Msi1, is not highly expressed in the SCN (Table 2). Two of the FSS genes that are MSI2 targets (Table 2) are not well understood (Blcap and Ntpcr), but are expressed abnormally in cancer cells (Pasdziernik et al., 2009; Gromova et al., 2017), which tend to be poorly differentiated.

MSI2 is categorized within the RNA binding motif containing (RBM) family of genes that expresses proteins containing the RNA recognition motif (RRM) (Birney et al., 1993) according to the HUGO Gene Nomenclature Committee at the European Bioinformatics Institute, https://www.genenames.org/cgi-bin/genefamilies/set/725. We examined the ABA for additional members of the RBM family that are highly expressed in the SCN (considered here as a Z-score greater than 1), and we identified additional gene candidates for future studies of RNA-binding activity in the circadian clock. Most notable is Celf3, which is expressed at higher levels in the SCN than in most other brain areas and, like MSI2, was included in the SCN FSS. Along with the Celf gene family, other RBM-containing proteins expressed in the SCN are from the Elavl, Rbm, and Rbfox families which are expressed at moderate levels (Table 2). The RNA-binding protein ELAVL1 (HuR) binds to and stimulates MSI2 activity. Inhibiting Rbm4 message coding for Lark protein impacts circadian rhythms (Kojima et al., 2007), and Rbfox3 codes for the NeuN marker protein of mature neurons that is expressed at unexpectedly low levels in much of the SCN, as mentioned previously.

3.5. Circadian rhythms persist in the SCN of brain slice cultures maintained in stem cell medium

The circadian clock within the SCN could regulate the differentiation and maturation of the developing or adult SCN, as indicated for neurosphere cultures made from mouse SVZ and DG (Malik et al., 2015a, b). Because epidermal stem cells show control by intrinsic circadian clocks (Janich et al., 2011), stem-like cells within the SCN may be capable of generating circadian rhythms. Experiments to explore this possibility would be enhanced if the SCN cells survive and the clock continues to function in a medium such as SPM that supports stem cells. It was also important to screen for any effects of this atypical culture condition on the SCN's circadian properties because the SCN explant cultures displayed altered morphology and differential cell survival in SPM. The question addressed was whether circadian clock cells continue to express a rhythm despite the presence of additional growth factors that are known to activate MAP kinase pathways or other SCN inputs that serve in synchronizing the clock to external 24-hour cycles.

BLI of three SCN brain slice cultures showed that circadian expression of the Per1 gene can persist in SPM (Fig. 5A&B), although the rhythm was severely disrupted in one culture (Fig. 5C). Period estimates for the two oldest animals were both 23 h based on peak-to-peak intervals, (Fig. 5A&B). In the SCN of the oldest animal, the circadian rhythm reached a maximum near the middle of the light phase (Fig. 5A), which is in agreement with earlier studies of Per2 gene expression (Nakamura et al., 2005). The previously described phase difference between ventral and dorsal SCN was also observed (Fig. 5B). However, the phase of the first peak in the rhythm from this animal's SCN was later than expected, when compared with the previous light/dark cycle, and there was an unexpected small, early peak in the signal during the first cycle of the right SCN (Fig. 5B). Both of these departures in the young SCN from the normal rhythm observed in the older SCN suggested that SPM disrupts but does not eliminate circadian rhythms. Much greater disruption was observed in the SCN from the youngest mouse (Fig. 5C). The SCN cultures also showed unexpected Per1 expression in areas ventrolateral (Fig. 5B) and dorsal (Fig. 5B&C) to the SCN. All three mice were males in the same litter of the inbred B6 strain, which minimized variability.

4. Discussion

4.1. The SCN expresses many proteins found in partially differentiated cells

The current results confirmed and extended previous descriptions of apparent partial cell differentiation in the SCN through phenotyping of SCN cells by ICC and cell survival and proliferation assays in SPM. These additional stem cell-like properties include expression of MSI2, nestin, OCT4, and vimentin in brain slices and explant cultures. Nestin, OCT4, and SOX2 colocalized with another stem cell marker protein, GFAP, that is also a marker of reactive astrocytes (Robel et al., 2011), suggesting a range of stem-like cell types survived in culture. Close examination of MSI2 expression showed that it was expressed in GFAP-positive cells resembling astrocytes and in numerous adjacent cells lacking GFAP including neurons. Earlier reports showed expression of SOX2, DCX, and DCX-like proteins in SCN neurons and unusually low expression of mature neuronal marker NeuN (Walker et al., 2007;

Geoghegan and Carter, 2008; Hoefflin and Carter, 2014; Saaltink et al., 2012). SCN cells expressing SOX2 with GFAP are most similar to the neurogenic stem cells of the DG and SVZ, whereas SOX2-positive cells lacking GFAP resemble progenitor cells (Ming and Song, 2011).

Our results with explant cultures showed colocalization of SOX2 and PCNA, indicating SOX2-positive cells proliferated, while neurons were lost through cell death. Additional evidence that the explants remained viable in SPM was provided by luciferase bioluminescence persisting for at least seven weeks. Removal of the ependymal cells and the optic chiasm of SCN explants before culture indicates presence of resident stem-like cells in the SCN rather than their origination in adjacent structures followed by migration into the SCN. SOX2 was also co-expressed with the intermediate filament vimentin found in stem cells (Nie et al., 2009). Survival and proliferation of stem cells in tumors and normal tissues is favored by low-oxygen conditions activating hypoxia-inducible factor-1 (HIF-1) (Bar et al., 2010). Similarly, the SCN explants in our study were treated like neurosphere cultures (Malik et al., 2015a) and maintained in standard culture dishes that favored stem-like cell growth but not neuron survival. In contrast, typical bioluminescence imaging experiments of SCN explant cultures lasting several days usually rely on conditions favoring oxygen exchange through a porous membrane support that holds the neural tissue in a thin film of medium. This interface culture method was employed here when imaging brain slices of *Per1::luc* mice containing the SCN to evaluate circadian rhythms. The circadian rhythm of bioluminescence persisted in two of the three cultures maintained in SPM but with a shifted phase and atypical Per1 expression dorsal to the SCN. The *Per1::luc* transgene expression observed within and outside the SCN indicates Per1 is not silenced by this culture medium and could have a function in the stem-like cells independent of its role in the circadian clock's timing mechanism, particularly in areas that do not appear to be rhythmic.

It is still not completely understood whether circadian rhythms persist in most adult (mesenchymal), embryonic, or induced pluripotent stem cells (Morse et al., 2003; Kimiwada et al., 2009; Yagita et al., 2010; Malik et al., 2015a). Circadian rhythms regulate stem cells of the epidermis (Janich et al., 2011), but appear to be lacking in NSCs of neurosphere cultures prepared from adult mouse SVZ and DG until the cells are induced to differentiate (Malik et al., 2015a, b). The current results show that this stem cell culture medium can support circadian rhythms. It could be a useful environment for testing which conditions are permissive for the circadian clock and whether individual neural stem cells or progenitors also generate rhythms. It is noteworthy that SCN circadian rhythms were observed despite the absence of the serum supplement B27 that is typically used to maintain neuron survival in circadian studies of brain slice cultures. Nevertheless, the results also show the limitations imposed on measuring circadian rhythms in cell or tissue explant cultures maintained in SPM. The observed disruptions in rhythms may be explained as a disturbance in the phase or coupling between the circadian pacemakers within the SCN cell population, while circadian rhythms may persist in individual cells. It is likely that there was a shift in the bioluminescence signal over time in SPM towards origination in other rhythmic cell types such as astrocytes, thereby distorting the rhythmic pattern recorded. Astrocytes could have survived in the SCN explants because of EGF in the SPM that may have stimulated astrocytes through their heparin-binding epidermal growth factor receptors (HBEGFR) that are part of the EGF receptor family. HBEGF has been used in a serum-free culture method for cortical astrocytes that, reportedly, maintains a gene expression pattern more like that of resident reactive astrocytes of the brain than astrocytes maintained in serum-based medium (Foo et al., 2011).

EGFR expression was shown previously to be scattered throughout the SCN and also concentrated dorsal to the SCN in the hypothalamic subparaventricular region where SCN neurons project (Ma et al., 1994; Kramer et al., 2001, 2003; Snodgrass-Belt et al., 2005). It was concluded that this pathway regulates the animal's circadian locomotor rhythms, and EGF signaling suppression reversibly blocks locomotor activity. Evidence indicates that, rather than EGF, this timing signal is mediated through TGF-alpha binding to EGFR (Kramer et al., 2003), thereby activating downstream mitogen-activated kinase pathways in the SCN (Hao and Schwaber, 2006). Both neurons and astrocytes of the hypothalamus express EGFR. EGFR expression in the hypothalamic arcuate nucleus undergoes dynamic changes at the time of first proestrus in primates (Ma et al., 1994), an alteration that might also occur in the SCN to modify expressed circadian rhythms. In contrast, very little is known about the role of FGF-2 (the other SPM growth factor) in adult hypothalamic cells or the circadian clock.

4.2. Partially differentiated SCN cells may provide developmental and adult neuroplasticity

SCN cells described in the current study showing nestin and GFAP co-expression resemble stem cells that undergo neurogenesis in the DG or SVZ (von Bohlen Und Halbach, 2007). These cells may be a type of astrocyte that is proposed to regulate neurogenesis through Notch signaling (Lebkuechner et al., 2015). In this model, based on single-cell phenotyping, astrocytes expressing SOX2 and cytoskeletal proteins GFAP, vimentin, and nestin control Notch signaling pathways that suppress differentiation. It is possible that the overlapping pattern of SOX2, GFAP, vimentin, and nestin expression we observed in SCN brain sections or explant cultures indicates astrocytes maintaining the SCN's stem-like state through this mechanism. Interestingly, loss of Notch signaling enables neurogenesis from astrocytes of the striatum (Magnusson et al., 2014). Furthermore, Notch signaling through glial cells has been implicated in regulating memory impairments from sleep loss in Drosophila (Miller et al., 2009). Note, however, that a previous immunochemical study of perfused tissue did not see co-expression of SOX2 with nestin or vimentin in mouse SCN (Pellegrino et al., 2018), whereas we observed about 5% of cells in explant cultures co-expressing SOX2 and vimentin.

The SCN's stem cell properties may enable its cell network of circadian oscillators to adaptively adjust rhythmic timing signals leaving the SCN. Clearly, GABA neurosecretion is important in forming the ensemble circadian rhythm along with synaptic transmission within and between large populations of neurons producing VIP, arginine vasopressin (AVP), GRP, and calretinin (CR) or calbindin (Moore and Silver, 1998; Jobst et al., 2004; Antle and Silver, 2005; Azzi et al., 2017). The substantial success with restoring circadian rhythms in SCN-ablated adult animals through embryonic SCN transplants may have been aided by a plasticity within the neural circuitry of the circadian timing system (Lehman et al., 1987; Silver et al., 1990). It is noteworthy that similar early transplantation studies using other brain regions were less successful at providing major recovery in animal models of Parkinson's disease (Bjorklund and Lindvall, 2017). The apparent lack of complete development of some SCN cells may enable them to further differentiate and grow adaptively in new microenvironments following various stressors like those impacting neural transplants. Transplant studies revealed SCN flexibility in how it conveys circadian signals in that synaptic or humoral signaling suffice (Silver et al., 1990).

Some of the apparent plasticity in SCN organization may have evolved because the SCN is a sensory structure receiving retinal input and uniquely engaged in providing precise daily timing to multiple behavioral and physiological processes. It provides sleep and metabolic regulation that can be impacted by shifting seasonal dawn and dusk and ongoing postnatal development. Critical in its production of accurate timing signals for the body is a prominent fiber tract from the optic nerve conveying photic information through direct excitatory glutamatergic synapses, making the SCN an important sensory area of the brain (Lokshin et al., 2015).

The stem-like cells described in the SCN resemble, to some extent, stem cells reported in the arcuate nucleus that have been suggested as serving in neuroplasticity needed for arcuate-dependent behavioral and physiological functions (McNay et al., 2012). Possible factors selecting

for SCN neural plasticity provided by partially differentiated cells includes transitions through life stages (e.g., sexual maturation, pregnancy or aging) and their differing metabolic demands on the organism. Because of the pivotal role of the SCN in many brain functions the stem-like cells may provide a plasticity in SCN circuitry to correct for external forces, such as responses to food scarcity or abundance associated with seasons and their differing day length and light intensity.

The SCN progenitor-like cells and cells resembling neuroblasts may complete their differentiation and form synapses that alter neural circuits responsible for adjusting key properties of circadian rhythms resulting from the SCN's coupled circadian oscillators (Herzog et al., 2004; Sun et al., 2017). These features of the clock include the period of the oscillation and its phase relative to the external cycle of light and darkness. As stem cells differentiate, cell junctions and direct communication between cells typically increase, e.g., through increased E-cadherin versus N-cadherin expression. Evidence indicates that changes in cell-cell communication occur rhythmically in the SCN (Prosser et al., 2003) and also alter the circadian period, which could represent an adaptive neural plasticity along with chemical synapse modifications (Azzi et al., 2017).

The importance of cell connectivity in SCN functions was also revealed in two recent meta-analyses of genes expressed preferentially in mouse SCN (Zhao et al., 2016; Brown et al., 2017). Interestingly, we examined the 20 most SCN-enriched genes reported by the first of these studies and found that nine have stem cell or developmental GO Biological Process designations: Ahl1, Calcr, Cckar, Chodl, Gpld1, Hap1, Ngb, Scn9a, and Zcchc12. In the second study a statistical method was used that minimizes effects from variance in gene expression on measures of gene importance in the SCN, and mouse RNA was collected at different times of day in the studies they included. The authors mention that these two factors combined to reduce representation of some rhythmic genes (Brown et al., 2017). Similarly, reliance on FSS data in our study may have also minimized inclusion of important SCN genes because these mice were sampled just after light onset, between 7 and 9 A M (Allen Brain Institute, personal communication), possibly selecting against rhythmic genes maximally expressed many hours later. Additionally, the ABA study was derived from only male adult mice. Nevertheless, Brown et al., who included data from adult females and multiple phases (Brown et al., 2017), did confirm the importance of two additional homeobox genes, Six3 and Six6, and four FSS genes expressed in the SCN (Avp, Lhx1, Rgs16, and Vipr2) in agreement with Beligala et al., 2018 (Zhao et al., 2016).

4.3. Elevated expression of stem cell marker MSI2 in the SCN suggests significant RNA processing occurs in circadian clock cells

Results provided here indicate MSI2 regulates 12 of the 46 genes in the FSS, including itself, providing evidence that it is a broad regulator of established as well as potentially important SCN gene products (Blcap, Flrt3, Msi2, Ntpcr, Pdcd4, Rgs16, Rorb, Rps6ka2, Slc5a3, Sox2, Trp53i11, Zfhx3). Many of these target genes have yet to be characterized in relation to the circadian clock. Recent reviews describe several RNA processing events regulated by and serving in circadian clocks throughout the body (Green, 2018; Torres et al., 2018). MSI2 is a master RNA-binding protein and posttranscriptional regulator that primarily controls mRNA stability and translation (Kudinov et al., 2017). It maintains the undifferentiated state of stem cells and cancer cells, serves in tissue regeneration, and is controlled through Notch pathways of stem cells (Takahashi et al., 2013; Kharas and Lengner, 2017). Although MSI2 and its isoform MSI1 are more commonly found in neoplastic cells (Kudinov et al., 2017), MSI2 is expressed throughout the SCN, as shown in the current study, within neurons and GFAP-positive astrocytes of SCN explant tissue before and after culture and in brain sections from perfused mice. This pattern confirms the elevated Msi2 RNA levels detected in SCN through ISH patterns depicted in the ABA and the inclusion of Msi2 in the SCN FSS (Zhao et al., 2016). MSI1 and MSI2 expression have been identified previously in reactive astrocytes and sites of adult neurogenesis in mouse brain (Sakakibara et al., 2001).

In summary of results in Table 2, highly likely MSI2 targets in the SCN include several of the core clock genes, about a fourth of FSS genes, 7 of 11 stem-like FSS genes, and 15 of the 29 stem cell genes examined. Interestingly, we did not find evidence of MSI2 targeting GFAP, nestin, or vimentin, suggesting that they may function upstream of MSI2. This result agrees with proposed astrocyte regulation of the stem-like state through Notch signaling (Lebkuechner et al., 2015), as mentioned above (Section 4.2), while Notch genes may also be under MSI2 control (Table 2). Although Notch was not highly expressed in the SCN, stem cell-regulators Wnt and Shh that interact with Notch pathways were (Table 2). Also, the GO Biological Processes of SCN FSS members Dlk1 and Slc35c1 include negative regulation of Notch signaling pathway.

The mRNA altered by Msi2 KO, KD, and OE has been described in several tissues: skin (Bennett et al., 2016; Ma et al., 2017), intestinal epithelium (Wang et al., 2015), hematopoietic stem cells (Park et al., 2014; Rentas et al., 2016; Kharas and Lengner, 2017). As summarized

Table 3
MSI2 knockout (KO), knockdown (KD), and overexpression (OE) studies.

Target tissue and methods	Reference	Major cellular effects	Major targets
Intestinal epithelium, colorectal cancer cell lines – CLIP-Seq; qRT-PCR	Wang et al. (2015)	KO: reduced intestinal epithelial cell proliferation KD: reduced colorectal cancer cell proliferation OE: increased intestinal epithelial proliferation	Pathways serving ribosomes, stem cells, metabolism, cell-cell communication, and neurodegenerative diseases
HSC, leukemia cell line – HITS-CLIP; RNA-Seq	Park et al. (2014)	KO: increased differentiation into progenitor cells; smaller quiescent cell population	TGFβ receptors; Numb; RNA metabolism and HSC self-renewal signaling pathways
HSC – HITS-CLIP; RNA-seq	Rentas et al. (2016)	KD: decreased cell number OE: increased HSC self-renewal	AHR signaling; TGFβ receptors; PER1, PER2, NR1D2, and ARNTL2
HSC, human leukemia cell lines – qRT-PCR	Kharas and Lengner (2017)	KD: depletes HSC population OE: accelerates HSC cell cycle	Numb; Wnt, Ras-MAPK, and Myc pathways
Skin, mouse keratinocytes – HITS-CLIP; RNA-seq; qPCR	Bennett et al. (2016)	KD: increases cell migration speed and focal adhesions	Notch pathway, focal adhesion, extracellular matrix-receptor interaction, regulation of actin and cytoskeleton, adherens junctions, cytokine-cytokine receptor interaction, and p53 signaling
Skin – CLIP-qPCR assay	Ma et al. (2017)	KO: enhances hair cycle OE: delays hair cycle, maintains hair follicle stem cell quiescence	Hh and its downstream targets Shh, Gli1 and Ptch2

HSC: mouse hematopoietic stem cells. HITS: high-throughput sequencing. CLIP: crosslinking immunoprecipitation. AHR: Aryl hydrocarbon receptor. TGFβ: transforming growth factor-β.

in Table 3, these studies describe MSI2 effects on cell differentiation, migration, and cell-cell interactions that may be relevant to any neurogenesis or circuit remodeling in the SCN. Cell-cell interactions are modified when cells dedifferentiate during EMT into a more stem-like state, typically producing more motile cells (Shibue and Weinberg, 2017). In the SCN, these physically altered cells may generate new neurites or undergo synaptic plasticity under the control of RNA-binding proteins (Sephton and Yu, 2015).

Numb suppression by MSI2 may help to maintain the immature phenotype of SCN cells. NUMB protein inhibits Notch and Wnt pathways (Cheng et al., 2008; Griner and Reuther, 2010). Similarly, the previously reported low SCN expression of NeuN, a protein marker of mature neurons resulting from Rbfox3 gene expression, has been explained as a result of alternative splicing of RNA from a closely related SCN gene (Partridge and Carter, 2017). Perhaps NeuN is expressed at low levels in some SCN neurons so that it does not induce differentiation and thereby impede MSI2 activity, which is known to suppress cell differentiation by inhibiting Numb (Table 3). MSI2 can also act independently of Numb, such as during fibroblast migration (Bennett et al., 2016), and Numb does not appear to be an important MSI2 target in hematopoietic stem cells (Park et al., 2014).

Another notable result from studies manipulating MSI2 levels is that MSI2 targets TGFβ receptor expression (Table 3). Expression of the core clock protein BMAL1 is increased by TGFβ in epithelial cells and fibroblasts of lung (Dong et al., 2016), whereas it suppresses Per1 and Per2 expression in NIH 3T3 fibroblasts (Gast et al., 2012). Interestingly, Rentas et al. also identified significant MSI2 targeting of PER1, PER2, NR1D2, and ARNTL2, suggesting effects on clock protein expression that should be examined further in the SCN.

MSI2 inhibits signaling through the aryl hydrocarbon receptor (AHR) in human hematopoietic stem cells (Rentas et al., 2016), and AHR is expressed in the SCN (Petersen et al., 2000). Several studies, but not all, link activation of AHR by exogenous ligands to changes in period or phase of circadian rhythms and altered core clock protein levels (Anderson et al., 2013). MSI2's regulation of the AHR pathway that in turn interacts with the circadian clock is another way it could modify rhythms. MSI2 also controls expression of AVP (Rentas et al., 2016), a major neuropeptide of SCN neurons (Cormier et al., 2015).

Although MSI1 and MSI2 may be redundant in some cells, they also have divergent functions: In astrocytes of the cerebrum MSI1 appears to control differentiation from multipotent SVZ progenitor cells (Sakakibara and Okano, 1997). MSI2 is a target of MSI1 RNA-binding in spermatogonia (Sutherland et al., 2015). Hematopoietic stem cells are disrupted by Msi2 gene KO, but do not show a compensatory increase in Msi1 expression (Park et al., 2014). Similarly, Msi1 is not required for developing mouse retina (Susaki et al., 2009), but its KD produces ependymal cell proliferation and disrupts stem cell production (Sakakibara et al., 2002).

A phylogenetic analysis of RRM-containing genes within the Metazoa indicates they are ancient (Birney et al., 1993). MSI2 and additional RBM family proteins CELF2, CIRBP, hnRNP Q, LARK, and RBMP4 may have been retained during evolution of the SCN circadian clock to maintain an adaptive plasticity in translational capabilities. Cirbp is expressed at moderate levels in SCN and in other brain areas according to its Z-score. It has a reported role in controlling circadian clock genes through RNA-binding (Liu et al., 2013). Similarly, the hnRNP Q gene (Syncrip) regulates circadian rhythms in clock proteins PER1 and CRY1 but was not highly expressed in SCN.

Interestingly, Cirbp and Notch transcripts are downregulated by MSI2 KO, whereas Per1 message is elevated (Park et al., 2014). The rhythmic activity of core circadian clock protein REV-ERB ALPHA may be regulated translationally by hnRNP Q, which is also under clock control (Kim et al., 2010), and hnRNP D represses stability of mRNA from core clock gene Cry1 (Woo et al., 2010). LARK protein expressed from Rbp4 and Rbp4a genes controls the period and amplitude of circadian rhythms in PER1 (Kojima et al., 2007). Although not significantly rhythmic at the RNA transcript level, LARK protein levels are under circadian control, which is one example of how transcriptional rhythms do not necessarily define circadian rhythms in protein levels or activity (Kojima et al., 2007).

Additional studies of the role of MSI2 and other RNA-binding proteins in the SCN should examine their RNA targets and protein partners further to evaluate molecular functions and whether these vary in response to circadian timing. For example, MSI2 interacts with SOX2 in glioma cells (Cox et al., 2013) and may operate rhythmically in stem-like SCN astrocytes or neurons. Although Msi2 expression shows circadian rhythms in liver and kidney (by CircaDB), a circadian rhythm was not detected in the SCN as a whole.

4.4. MSI2 may control SCN cells by regulating miRNA

It has been estimated that an individual microRNA (miRNA) can control hundreds of genes, and miRNAs may control about a third of all genes (Thomas et al., 2010). MSI2 is a strong candidate for high-level control of SCN miRNAs. MSI2 interacts with proteins of the ELAVL (Hu) RNA-binding protein family that function in synaptic plasticity and addiction (Bryant and Yazdani, 2016). ELAVL1 forms a complex with MSI2 that controls miR-7 in nervous system development and regulates miRNAs distribution (Choudhury et al., 2013; Doxakis, 2014; Meza-Sosa et al., 2014; Loffreda et al., 2015).

Activity of the core clock genes Per1 and Per2 is altered by miR-132 and miR-219, producing effects on the rhythm's period and its phase shifts in response to entraining light signals (Cheng and Obrietan, 2007). According to the online Mouse Genome Database (MGD, http://www.informatics.jax.org/), MSI2 and ELAVL1 could alter the circadian clock through miRNA because they are predicted to bind and suppress miR-7, miR-132, and miR-219. Also, miR-7 and miR-219 influence voltage-gated K^+ channels, NMDA-type receptors, and intracellular Ca^{2+}, potentially altering neuronal circadian rhythms (Mehta and Cheng, 2013). Like the circadian clock mechanism, evidence indicates ELAVL1 is regulated by pyruvate kinase in glioblastoma cells (Mukherjee et al., 2016), suggesting another way that energy demands within the organism might also alter SCN cell networks. Alternatively, ELAVL1 may serve in a non-clock function in the SCN by preventing excitotoxic damage though intracellular Ca^{2+} (Skliris et al., 2015); the SCN is unique among hypothalamic nuclei in receiving substantial glutamatergic retinal afferents, and protection from excessive sensory stimuli would be expected.

4.5. Stem-like cells persist in SCN explant cultures made from mice of different mouse strains and across a wide age range

Mice between 6 and 56 weeks old were used to prepare SCN explant cultures for ICC. Although adult neural stem cell activity generally declines with age, stem-like cells of the SCN persisted in these cultures. Explant cultures prepared from mice of different genetic backgrounds indicated stem-like SCN cells are not limited to B6 mice and are likely found in other species. A publication that appeared after our work was completed, provided evidence that the adult human SCN contains stem-like cells, suggesting that this may be a general property of the brain clock (Pellegrino et al., 2018). Studies exploring what factors maintain the immature state of SCN cells are aided by the knowledge that circadian rhythms persist in SPM; interaction between circadian clock components and stem cell-related genes may provide insight into cell differentiation.

The B6 mouse line provided most of the SCN explant cultures. It offers the possibility of propagating and differentiating many SCN cells from explant cultures derived from mice of the same genetic background, thereby reducing variability in resulting data. Following differentiation, circadian properties of neurons and astrocytes could be examined in conventional culture medium. The cell line SCN 2.2 was developed from immortalized fetal rat SCN and has served in many

circadian studies of neurons and glia (Earnest et al., 1999; Allen and Earnest, 2002; Farnell et al., 2011; Eggleton et al., 2016). Generating a cell line from adult mouse SCN would enable studies to fully benefit from mouse genome data and allow the circadian clock to be examined in cell lines produced from individual animals following specific mutations and epigenetic or developmental alterations. Further studies of MSI2 and related RNA-binding proteins in SCN cells could determine whether they provide a molecular switch regulating the persistent immature SCN state. The SCN, olfactory bulb, arcuate nucleus, hippocampus, and cerebellum are arguably the most well recognized brain areas containing a self-sustaining circadian clock (Piggins and Guilding, 2011). Interestingly, these structures are also rich in cells expressing stem-cell related genes, many of which were examined here.

5. Conclusions

SOX2, OCT4, MSI2, nestin, and vimentin expression, and cellular co-localization of several of these proteins with GFAP provides additional evidence that diverse stem-like cells remain in the adult SCN following early development. Stem-like cells expressing these proteins proliferate coincidentally with neuronal loss in SCN explants maintained under culture conditions favorable for undifferentiated cell survival. This stem cell medium alters but does not eliminate SCN circadian rhythms. SCN cells positive for OCT4, nestin or SOX2 but negative for GFAP suggest that SCN explants contain progenitor cells that could differentiate further, ultimately producing neurons or glial cells. The high percentage of SCN cells positive for MSI2 provides evidence for RNA-binding proteins serving an important but uncharacterized role in the stem-like state of circadian cells.

Declarations of interest

None.

Acknowledgements

Funding: This work was supported by NSF grants 1256105 and 1749500 to RS and a Building Strength Grant from BGSU to MG. The funding sources had no involvement in study design; in the collection, analysis and interpretation of data; in the writing of the report; or in the decision to submit the article for publication.

Appendix A. Supplementary data

Supplementary material related to this article can be found, in the online version, at doi:https://doi.org/10.1016/j.ijdevneu.2019.04.007.

References

Allen, G.C., Earnest, D.J., 2002. Real-time analysis of rhythmic gene expression in immortalized suprachiasmatic nucleus cells. Neuroreport 13 (16), 2027–2030.
Anderson, G., Beischlag, T.V., et al., 2013. The circadian clock circuitry and the AHR signaling pathway in physiology and pathology. Biochem. Pharmacol. 85 (10), 1405–1416.
Antle, M.C., Silver, R., 2005. Orchestrating time: arrangements of the brain circadian clock. Trends Neurosci. 28 (3), 145–151.
Azzi, A., Evans, J.A., et al., 2017. Network dynamics mediate circadian clock plasticity. Neuron 93 (2), 441–450.
Bar, E.E., Lin, A., et al., 2010. Hypoxia increases the expression of stem-cell markers and promotes clonogenicity in glioblastoma neurospheres. Am. J. Pathol. 177 (3), 1491–1502.
Beligala, D.H., De, A., et al., 2018. A Meta-Analysis Characterizing Stem-Like Gene Expression in the Suprachiasmatic Nucleus and Its Circadian Clock. Biomed Res. Int. 2018, 3610603.
Bennett, C.G., Riemondy, K., et al., 2016. Genome-wide analysis of Musashi-2 targets reveals novel functions in governing epithelial cell migration. Nucleic Acids Res. 44 (8), 3788–3800.
Birney, E., Kumar, S., et al., 1993. Analysis of the RNA-recognition motif and RS and RGG domains: conservation in metazoan pre-mRNA splicing factors. Nucleic Acids Res. 21 (25), 5803–5816.
Bjorklund, A., Lindvall, O., 2017. Replacing Dopamine Neurons in Parkinson's Disease: How did it happen? J. Parkinsons Dis. 7 (s1), S21–S31.
Brown, L.A., Williams, J., et al., 2017. Meta-analysis of transcriptomic datasets identifies genes enriched in the mammalian circadian pacemaker. Nucleic Acids Res. 45 (17), 9860–9873.
Bryant, C.D., Yazdani, N., 2016. RNA-binding proteins, neural development and the addictions. Genes Brain Behav. 15 (1), 169–186.
Cheng, H.Y., Obrietan, K., 2007. Revealing a role of microRNAs in the regulation of the biological clock. Cell Cycle 6 (24), 3034–3035.
Cheng, X., Huber, T.L., et al., 2008. Numb mediates the interaction between Wnt and Notch to modulate primitive erythropoietic specification from the hemangioblast. Development 135 (20), 3447–3458.
Choudhury, N.R., de Lima Alves, F., et al., 2013. Tissue-specific control of brain-enriched miR-7 biogenesis. Genes Dev. 27 (1), 24–38.
Cormier, H.C., Della-Maggiore, V., et al., 2015. Suprachiasmatic vasopressin and the circadian regulation of voluntary locomotor behavior. Eur. J. Neurosci. 41 (1), 79–88.
Cox, J.L., Wilder, P.J., et al., 2013. The SOX2-interactome in brain cancer cells identifies the requirement of MSI2 and USP9X for the growth of brain tumor cells. PLoS One 8 (5), e62857.
Dong, C., Gongora, R., et al., 2016. Regulation of transforming growth factor-beta1 (TGF-beta1)-induced pro-fibrotic activities by circadian clock gene BMAL1. Respir. Res. 17, 4.
Doxakis, E., 2014. RNA binding proteins: a common denominator of neuronal function and dysfunction. Neurosci. Bull. 30 (4), 610–626.
Earnest, D.J., Liang, F.Q., et al., 1999. Immortal time: circadian clock properties of rat suprachiasmatic cell lines. Science 283 (5402), 693–695.
Eggleton, P., Bremer, E., et al., 2016. Calreticulin, a therapeutic target? Expert Opin. Ther. Targets 20 (9), 1137–1147.
Farnell, Y.F., Shende, V.R., et al., 2011. Immortalized cell lines for real-time analysis of circadian pacemaker and peripheral oscillator properties. Eur. J. Neurosci. 33 (8), 1533–1540.
Foo, L.C., Allen, N.J., et al., 2011. Development of a method for the purification and culture of rodent astrocytes. Neuron 71 (5), 799–811.
Gast, H., Gordic, S., et al., 2012. Transforming growth factor-beta inhibits the expression of clock genes. Ann. N. Y. Acad. Sci. 1261, 79–87.
Geoghegan, D., Carter, D.A., 2008. A novel site of adult doublecortin expression: neuropeptide neurons within the suprachiasmatic nucleus circadian clock. BMC Neurosci. 9, 2.
Green, C.B., 2018. Circadian posttranscriptional regulatory mechanisms in mammals. Cold Spring Harb. Perspect. Biol. 10 (6).
Griner, L.N., Reuther, G.W., 2010. Aggressive myeloid leukemia formation is directed by the Musashi 2/Numb pathway. Cancer Biol. Ther. 10 (10), 979–982.
Gromova, I., Svensson, S., et al., 2017. Identification of BLCAP as a novel STAT3 interaction partner in bladder cancer. PLoS One 12 (11), e0188827.
Hao, H., Schwaber, J., 2006. Epidermal growth factor receptor induced Erk phosphorylation in the suprachiasmatic nucleus. Brain Res. 1088 (1), 45–48.
Herzog, E.D., Aton, S.J., et al., 2004. Temporal precision in the mammalian circadian system: a reliable clock from less reliable neurons. J. Biol. Rhythms 19 (1), 35–46.
Hiler, D.J., Bhattacherjee, A., et al., 2008. Circadian mPer1 gene expression in mesencephalic trigeminal nucleus cultures. Brain Res. 1214, 84–93.
Hoefflin, S., Carter, D.A., 2014. Neuronal expression of SOX2 is enriched in specific hypothalamic cell groups. J. Chem. Neuroanat. 61-62, 153–160.
Iwai, S., Takeda, M., 2007. Expression analysis of two types of transcripts from circadian output gene lark in Bombyx mori. Comp. Biochem. Physiol. B, Biochem. Mol. Biol. 146 (4), 470–476.
Janich, P., Pascual, G., et al., 2011. The circadian molecular clock creates epidermal stem cell heterogeneity. Nature 480 (7376), 209–214.
Jobst, E.E., Robinson, D.W., et al., 2004. Potential pathways for intercellular communication within the calbindin subnucleus of the hamster suprachiasmatic nucleus. Neuroscience 123 (1), 87–99.
Kharas, M.G., Lengner, C.J., 2017. Stem cells, Cancer, and MUSASHI in blood and guts. Trends Cancer 3 (5), 347–356.
Kim, D.Y., Woo, K.C., et al., 2010. hnRNP Q and PTB modulate the circadian oscillation of mouse Rev-erb alpha via IRES-mediated translation. Nucleic Acids Res. 38 (20), 7068–7078.
Kimiwada, T., Sakurai, M., et al., 2009. Clock genes regulate neurogenic transcription factors, including NeuroD1, and the neuronal differentiation of adult neural stem/progenitor cells. Neurochem. Int. 54 (5-6), 277–285.
Kojima, S., Matsumoto, K., et al., 2007. LARK activates posttranscriptional expression of an essential mammalian clock protein, PERIOD1. Proc Natl Acad Sci U S A 104 (6), 1859–1864.
Kramer, A., Yang, F.C., et al., 2001. Regulation of daily locomotor activity and sleep by hypothalamic EGF receptor signaling. Science 294 (5551), 2511–2515.
Kramer, A., Yang, F.C., et al., 2003. Regulation of daily locomotor activity and sleep by hypothalamic EGF receptor signalling. Novartis Found. Symp. 253, 250–262 discussion 102-259, 263-256, 281-254.
Kudinov, A.E., Karanicolas, J., et al., 2017. Musashi RNA-Binding Proteins as Cancer Drivers and Novel Therapeutic Targets. Clin. Cancer Res. 23 (9), 2143–2153.
Lebkuechner, I., Wilhelmsson, U., et al., 2015. Heterogeneity of Notch signaling in astrocytes and the effects of GFAP and vimentin deficiency. J. Neurochem. 135 (2), 234–248.
Lehman, M.N., Silver, R., et al., 1987. Circadian rhythmicity restored by neural transplant. Immunocytochemical characterization of the graft and its integration with the host brain. J. Neurosci. 7 (6), 1626–1638.
Lein, E.S., Hawrylycz, M.J., et al., 2007. Genome-wide atlas of gene expression in the adult mouse brain. " Nature 445 (7124), 168–176.

Lindley, J., Deurveilher, S., et al., 2008. Transforming growth factor-alpha and glial fibrillary acidic protein in the hamster circadian system: daily profile and cellular localization. Brain Res. 1197, 94–105.
Liu, Y., Hu, W., et al., 2013. Cold-induced RNA-binding proteins regulate circadian gene expression by controlling alternative polyadenylation. Sci. Rep. 3, 2054.
Liu, D., Stowie, A., et al., 2018. mTOR signaling in VIP neurons regulates circadian clock synchrony and olfaction. Proc Natl Acad Sci U S A 115 (14), E3296–E3304.
Loffreda, A., Rigamonti, A., et al., 2015. RNA-Binding Proteins in the Regulation of miRNA Activity: A Focus on Neuronal Functions. Biomolecules 5 (4), 2363–2387.
Lokshin, M., LeSauter, J., et al., 2015. Selective distribution of retinal input to mouse SCN revealed in analysis of sagittal sections. J. Biol. Rhythms 30 (3), 251–257.
Ma, Y.J., Hill, D.F., et al., 1994. "Expression of epidermal growth factor receptor changes in the hypothalamus during the onset of female puberty. Mol. Cell. Neurosci. 5 (3), 246–262.
Ma, X., Tian, Y., et al., 2017. Msi2 Maintains Quiescent State of Hair Follicle Stem Cells by Directly Repressing the Hh Signaling Pathway. J. Invest. Dermatol. 137 (5), 1015–1024.
Magnusson, J.P., Goritz, C., et al., 2014. A latent neurogenic program in astrocytes regulated by Notch signaling in the mouse. Science 346 (6206), 237–241.
Malik, A., Jamasbi, R.J., et al., 2015a. Development of circadian oscillators in neurosphere cultures during adult neurogenesis. PLoS One 10 (3), e0122937.
Malik, A., Kondratov, R.V., et al., 2015b. Circadian clock genes are essential for normal adult neurogenesis, differentiation, and fate determination. PLoS One 10 (10), e0139655.
McNay, D.E., Briancon, N., et al., 2012. Remodeling of the arcuate nucleus energy-balance circuit is inhibited in obese mice. J. Clin. Invest. 122 (1), 142–152.
Mehta, N., Cheng, H.Y., 2013. Micro-managing the circadian clock: the role of microRNAs in biological timekeeping. J. Mol. Biol. 425 (19), 3609–3624.
Meza-Sosa, K.F., Pedraza-Alva, G., et al., 2014. microRNAs: key triggers of neuronal cell fate. Front. Cell. Neurosci. 8, 175.
Michelucci, A., Bithell, A., et al., 2016. The neurogenic potential of astrocytes is regulated by inflammatory signals. Mol. Neurobiol. 53 (6), 3724–3739.
Migaud, M., Butrille, L., et al., 2015. Seasonal regulation of structural plasticity and neurogenesis in the adult mammalian brain: focus on the sheep hypothalamus. Front. Neuroendocrinol. 37, 146–157.
Miller, W.J., Leventhal, I., et al., 2009. Mechanically induced reactive gliosis causes ATP-mediated alterations in astrocyte stiffness. J. Neurotrauma 26 (5), 789–797.
Ming, G.L., Song, H., 2011. Adult neurogenesis in the mammalian brain: significant answers and significant questions. Neuron 70 (4), 687–702.
Mohr, M.A., DonCarlos, L.L., et al., 2017. Inhibiting production of new brain cells during puberty or adulthood blunts the hormonally induced surge of luteinizing hormone in female rats. eNeuro 4 (5).
Moore, R.Y., Silver, R., 1998. Suprachiasmatic nucleus organization. Chronobiol. Int. 15 (5), 475–487.
Morse, D., Cermakian, N., et al., 2003. No circadian rhythms in testis: Period1 expression is clock independent and developmentally regulated in the mouse. Mol. Endocrinol. 17 (1), 141–151.
Mukherjee, J., Ohba, S., et al., 2016. PKM2 uses control of HuR localization to regulate p27 and cell cycle progression in human glioblastoma cells. Int. J. Cancer 139 (1), 99–111.
Nakamura, W., Yamazaki, S., et al., 2005. Differential response of Period 1 expression within the suprachiasmatic nucleus. J. Neurosci. 25 (23), 5481–5487.
Nie, J., Wu, Q., et al., 2009. Ectopic expression of Ligand-of-Numb protein X promoted TGF-beta induced epithelial to mesenchymal transition of proximal tubular epithelial cells. Biochim. Biophys. Acta 1792 (2), 122–131.
Park, S.M., Deering, R.P., et al., 2014. Musashi-2 controls cell fate, lineage bias, and TGF-beta signaling in HSCs. J. Exp. Med. 211 (1), 71–87.
Partridge, L.M.M., Carter, D.A., 2017. Novel Rbfox2 isoforms associated with alternative exon usage in rat cortex and suprachiasmatic nucleus. Sci. Rep. 7 (1), 9929.
Pasdziernik, M., Kaltschmidt, B., et al., 2009. On the cytotoxicity of HCR-NTPase in the neuroblastoma cell line SH-SY5Y. BMC Res. Notes 2, 102.
Pellegrino, G., Trubert, C., et al., 2018. A comparative study of the neural stem cell niche in the adult hypothalamus of human, mouse, rat and gray mouse lemur (Microcebus murinus). J. Comp. Neurol. 526 (9), 1419–1443.
Petersen, S.L., Curran, M.A., et al., 2000. Distribution of mRNAs encoding the arylhydrocarbon receptor, arylhydrocarbon receptor nuclear translocator, and arylhydrocarbon receptor nuclear translocator-2 in the rat brain and brainstem. J. Comp. Neurol. 427 (3), 428–439.
Piggins, H.D., Guilding, C., 2011. The neural circadian system of mammals. Essays Biochem. 49 (1), 1–17.
Pizarro, A., Hayer, K., et al., 2013. CircaDB: a database of mammalian circadian gene expression profiles. Nucleic Acids Res. 41 (Database issue), D1009–1013.
Prosser, R.A., Rutishauser, U., et al., 2003. Intrinsic role of polysialylated neural cell adhesion molecule in photic phase resetting of the Mammalian circadian clock. J. Neurosci. 23 (2), 652–658.
Rentas, S., Holzapfel, N., et al., 2016. Musashi-2 attenuates AHR signalling to expand human haematopoietic stem cells. Nature 532 (7600), 508–511.
Robel, S., Berninger, B., et al., 2011. The stem cell potential of glia: lessons from reactive gliosis. Nat. Rev. Neurosci. 12 (2), 88–104.
Saaltink, D.J., Havik, B., et al., 2012. Doublecortin and doublecortin-like are expressed in overlapping and non-overlapping neuronal cell population: implications for neurogenesis. J. Comp. Neurol. 520 (13), 2805–2823.
Sakakibara, S., Okano, H., 1997. Expression of neural RNA-binding proteins in the postnatal CNS: implications of their roles in neuronal and glial cell development. J. Neurosci. 17 (21), 8300–8312.
Sakakibara, S., Nakamura, Y., et al., 2001. Rna-binding protein Musashi2: developmentally regulated expression in neural precursor cells and subpopulations of neurons in mammalian CNS. J. Neurosci. 21 (20), 8091–8107.
Sakakibara, S., Nakamura, Y., et al., 2002. RNA-binding protein Musashi family: roles for CNS stem cells and a subpopulation of ependymal cells revealed by targeted disruption and antisense ablation. Proc Natl Acad Sci U S A 99 (23), 15194–15199.
Sephton, C.F., Yu, G., 2015. The function of RNA-binding proteins at the synapse: implications for neurodegeneration. Cell. Mol. Life Sci. 72 (19), 3621–3635.
Shibue, T., Weinberg, R.A., 2017. EMT, CSCs, and drug resistance: the mechanistic link and clinical implications. Nat. Rev. Clin. Oncol. 14 (10), 611–629.
Silver, R., Lehman, M.N., et al., 1990. Dispersed cell suspensions of fetal SCN restore circadian rhythmicity in SCN-lesioned adult hamsters. Brain Res. 525 (1), 45–58.
Skliris, A., Papadaki, O., et al., 2015. Neuroprotection requires the functions of the RNA-binding protein HuR. Cell Death Differ. 22 (5), 703–718.
Snodgrass-Belt, P., Gilbert, J.L., et al., 2005. Central administration of transforming growth factor-alpha and neuregulin-1 suppress active behaviors and cause weight loss in hamsters. Brain Res. 1038 (2), 171–182.
Sofroniew, M.V., Vinters, H.V., 2010. Astrocytes: biology and pathology. Acta Neuropathol. 119 (1), 7–35.
Sun, J., Mu, H., et al., 2017. Calreticulin: a potential anti-cancer therapeutic target. Pharmazie 72 (9), 503–510.
Susaki, K., Kaneko, J., et al., 2009. Musashi-1, an RNA-binding protein, is indispensable for survival of photoreceptors. Exp. Eye Res. 88 (3), 347–355.
Sutherland, J.M., Sobinoff, A.P., et al., 2015. RNA binding protein Musashi-1 directly targets Msi2 and Erh during early testis germ cell development and interacts with IPO5 upon translocation to the nucleus. FASEB J. 29 (7), 2759–2768.
Takahashi, T., Suzuki, H., et al., 2013. Musashi-1 post-transcriptionally enhances phosphotyrosine-binding domain-containing m-Numb protein expression in regenerating gastric mucosa. PLoS One 8 (1), e53540.
Thomas, M., Lieberman, J., et al., 2010. Desperately seeking microRNA targets. Nat. Struct. Mol. Biol. 17 (10), 1169–1174.
Torres, M., Becquet, D., et al., 2018. Circadian processes in the RNA life cycle. Wiley Interdiscip. Rev. RNA 9 (3), e1467.
VanDunk, C., Hunter, L.A., et al., 2011. Development, maturation, and necessity of transcription factors in the mouse suprachiasmatic nucleus. J. Neurosci. 31 (17), 6457–6467.
von Bohlen, Und, Halbach, O., 2007. Immunohistological markers for staging neurogenesis in adult hippocampus. Cell Tissue Res. 329 (3), 409–420.
Walker, T.L., Yasuda, T., et al., 2007. The doublecortin-expressing population in the developing and adult brain contains multipotential precursors in addition to neuronal-lineage cells. J. Neurosci. 27 (14), 3734–3742.
Wang, S., Li, N., et al., 2015. Transformation of the intestinal epithelium by the MSI2 RNA-binding protein. Nat. Commun. 6, 6517.
Woo, K.C., Ha, D.C., et al., 2010. Circadian amplitude of cryptochrome 1 is modulated by mRNA stability regulation via cytoplasmic hnRNP D oscillation. Mol. Cell. Biol. 30 (1), 197–205.
Wu, S.H., Hang, L.W., et al., 2010. Curcumin induces apoptosis in human non-small cell lung cancer NCI-H460 cells through ER stress and caspase cascade- and mitochondria-dependent pathways. Anticancer Res. 30 (6), 2125–2133.
Yagita, K., Horie, K., et al., 2010. Development of the circadian oscillator during differentiation of mouse embryonic stem cells in vitro. Proc Natl Acad Sci U S A 107 (8), 3846–3851.
Yoo, S., Blackshaw, S., 2018. Regulation and function of neurogenesis in the adult mammalian hypothalamus. Prog. Neurobiol.
Zhao, G., Han, X., et al., 2016. Curcumin induces autophagy, inhibits proliferation and invasion by downregulating AKT/mTOR signaling pathway in human melanoma cells. Oncol. Rep. 35 (2), 1065–1074.